NASA CR-165383

NASA

ION BEAM MICROTEXTURING OF SURFACES

PREPARED FOR

LEWIS RESEARCH CENTER

NATIONAL AERONAUTICS AND SPACE ADMINISTRATION

GRANT NAG 3-43

Annual Report

May 1981

Raymond S. Robinson

Department of Physics
Colorado State University
Fort Collins, Colorado

1. Report No.	2. Government Accession No.	3. Recipient's Catalog No.
CR-165383		

4. Title and Subtitle	5. Report Date
Ion Beam Microtexturing of Surfaces (U)	May 1981
	6. Performing Organization Code

7. Author(s)	8. Performing Organization Report No.
Raymond S. Robinson	
	10. Work Unit No.

9. Performing Organization Name and Address	11. Contract or Grant No.
Physics Department Colorado State University Fort Collins, Colorado 80523	NAG 3-43
	13. Type of Report and Period Covered

12. Sponsoring Agency Name and Address	Contract Report
National Aeronautics and Space Administration Washington, DC 20546	14. Sponsoring Agency Code

15. Supplementary Notes

Grant Manager: Bruce A. Banks
NASA Lewis Research Center
Cleveland, OH 44135

16. Abstract

Some recent work in surface microtexturing by ion beam sputtering is described. The texturing is accomplished by deposition of an impurity onto a substrate while simultaneously bombarding it with an ion beam. A summary of the theory regarding surface diffusion of impurities and the initiation of cone formation is provided. Detailed experimental study of the time-development of individual sputter cones is described for the first time. A quasi-liquid coating has been observed that apparently reduces the sputter rate of the body of a cone compared to the bulk material. Experimental measurements of surface diffusion activation energies are presented for a variety of substrate-seed combinations and range from about 0.3 eV to 1.2 eV. Observations of apparent crystal structure in sputter cones are discussed. Measurements of the critical temperature for cone formation are also given along with a correlation of critical temperature with substrate sputter rate.

17. Key Words (Suggested by Author(s))		18. Distribution Statement
Texturing	Ion Beam	Unclassified, unlimited
Sputtering	Ion Source	
Microtexturing	Seeding	

19. Security Classif. (of this report)	20. Security Classif. (of this page)	21. No. of Pages	22. Price*

* For sale by the National Technical Information Service, Springfield, Virginia 22161

NASA-C-168 (Rev. 10-75)

N81-32982#

TABLE OF CONTENTS

I. INTRODUCTION

Textures can develop on solid surfaces in several ways during directed ion beam sputtering. Physical sputtering of solid materials, which is customarily accomplished using chemically inert ion species, can reveal individual crystal grains because of differential sputter etch rates dependent on crystal grain orientation. Impurities, precipitates, phases or initially irregular surfaces can also cause characteristic textures to develop during sputtering because of preferential etching of high sputter yield sites.[1] In addition, reactive ion beam etching can chemically texture a surface through selective removal of elements from an alloy.[2]

Of particular interest in this report, however, is the texturing induced by the deliberate deposition of an impurity material onto a solid surface while simultaneously bombarding the surface with an ion beam. This technique is often referred to as "seeding", with the impurity being termed the seed material. Under appropriate conditions, microscopic cones or hillocks develop because of preferential sputtering of surrounding material. It is generally understood that these cones are initiated by clusters of seed atoms protecting the underlying substrate while surrounding substrate material is etched away. Extensive experimental studies of seeding and ion beam texturing of surfaces have been reported earlier.[2]

Ion beam texturing has been attempted with many material combinations and has several potential applications. Textured surfaces have been successfully used for enhanced absorption of radiant energy in solar collectors.[4] Perhaps one of the more promising applications is in the realm of biomedical materials such as prostheses with soft or hard

tissue interfaces that require firm bonding.[5,6,7,8] Textured surfaces are also of interest for high reliability heat transfer surfaces[9] as well as high-field electron emitters for traveling wave tubes[10] and other applications including depression of secondary electron emission.[11]

Experimentally, results have been obtained in the following areas: time development of individual cones, study of a liquid-like coating on cones, activation energies for surface diffusion, the crystalline nature of cones, critical temperature as a function of substrate etch rates, texturing of additional materials and identification of cone failure mechanisms.

A bibliography is included as an appendix listing publications in the areas of surface texturing, sputtering, and some other topics related to the basic processes involved in ion beam microtexturing.

Experimental work under this Grant including operation of the scanning electron microscope has been carried out primarily by Stephen M. Rossnagel, a physics graduate student at Colorado State University.

II. THEORY

It has been postulated that the formation and replenishment of seed clusters is a result of the surface diffusion or migration of seed atoms with nucleation or attachment occurring when other seed atoms are encountered. It has also been widely believed that a necessary, but possibly not a sufficient, condition for the formation of sputter cones is that the seed material must have a lower sputter yield than the substrate material to account for the observed differential etch. Both the analytical model and subsequent experiments[12] showed that lower sputter yield of the seed material itself was not necessary for texturing to occur. Prior to the development of the model described below, though, knowledge of texturing was typically qualitative in nature, with only moderate ability to predict results prior to conducting the experiments.[3] The model discussed below is treated in greater detail elsewhere;[12,13] only a brief sketch will be provided here.

Diffusion Model

The migration of seed atoms along the surface was viewed as a random walk process. The random-walk diffusion length r_d was given by

$$r_d = (E_d/2m_s)^{1/4} \, (a_o/R_i Y_a \sigma_a)^{1/2} \exp\,(-E_d/2kT) \,, \qquad (1)$$

where E_d is the activation energy for the surface diffusion, k is Boltzmann's constant, T is the substrate temperature, m_s is the seed atom mass, a_o is mean distance between adsorption sites, R_i is the ion arrival rate, σ_a is the cross section of the adsorbed atoms for sputtering and Y_a is the sputter yield of the adsorbed atoms. This model

assumes that for the seed atoms to have sufficient mobility to gather into clusters, they should be bonded weakly to the substrate, compared to the mutual bonding of substrate atoms. The characteristic time for a seed atom to jump between adsorption sites is thus governed by the weak adsorption bonding, rather than the substrate lattice vibrations to which it is only loosely coupled.

A distance equal to twice the average diffusion radius is used as a measure of the average separation between clusters. If clusters were, on the average, much farther apart than $2r_d$, more clusters would begin to nucleate and grow in the intervening spaces where seed densities were enhanced, thus narrowing the gaps between clusters. At the other extreme, if clusters began to nucleate at separations much less than $2r_d$, larger clusters would grow faster and intercept diffusing seed material at the expense of smaller clusters. Thus, an average cluster separation of about $2r_d$ would be expected to be stable.

Seed Clustering

There is a critical size of a seed cluster, below which steady growth is not possible.[14] This critical radius is essentially the same value as is used in nucleation theory. It is obtained by setting to zero the derivative of free energy (surface plus volume) with respect to radius.[15] Continuous growth can take place above this radius, but dissociation of the cluster will tend to occur at smaller radii.

Whether or not a seed cluster is stable therefore depends on the diffusion rate to the cluster being sufficient, or insufficient, to supply the sputtering loss from a cluster of critical radius. To determine the stability requirements of seed clusters, it is necessary

to investigate more closely the processes of seed movement and clustering while adsorbed on a substrate.

Seed atoms are assumed to move from adsorption site to adsorption site on the surface by a random walk process. Only those seed atoms that acquire an energy greater than E_d are mobile. Energy is exchanged between seed atoms and the lattice through the loose coupling of the seed atom to thermal lattice vibrations bringing the adsorbed seed atom population into approximate thermal equilibrium with the substrate lattice. It is thus the temperature of the substrate that governs the fraction of seed atoms that are mobile at any given time. A random walk process for seed motion requires that, on the average, seed atoms experience an inelastic "collision" as a result of each jump to a neighboring adsorption site. The energy loss in the inelastic process would then be associated with a loss of the initial direction of motion resulting in a random direction for the next jump.

Detailed analysis of the process of seed diffusion and clustering yields an expression for the diffusion radius required to sustain a cluster of radius r_c and sputter yield Y_c

$$r_d = r_c \left[(Y_c - F_s)/F_s\right]^{1/2} \tag{2}$$

where F_s is the dimensionless ratio of seed atom arrival rate to beam ion arrival rate.

This diffusion radius is equated to the radius required to sustain a cluster to determine the minimum substrate temperature T_c that will give the required diffusion to sustain clusters of the minimum size.

$$T_c = E_d k \ell n \left[(E_d/2m_s)^{1/2} \; F_s N_o^{1/3} / R_i Y_a r_c^2 (Y_c - F_s) \right] \qquad (3)$$

Some of the physical effects following from the cone seeding theory can be directly investigated experimentally. After sputtering while seeding, scanning electron micrographs can be obtained of the sample surfaces. The average separation between cones is $(A/N)^{1/2}$, where N is the number of cones counted in an area A of the micrograph. The quantity <r>, one-half the average experimentally measured separation between cones, is identified with the diffusion radius r_d in the theoretical model. If <r> is plotted as a function of reciprocal temperature, a straight lines in expected on these plots. This can be shown by rewriting the expression for r_d as

$$r_d = r_o \exp(-E_d/2kT) \qquad (4)$$

where r_o is a constant

$$r_o = (E_d/2m_s)^{1/4} \; (a_o/R_i Y_a \sigma_a)^{1/2} \quad . \qquad (5)$$

Taking the natural logarithm and rearranging the result,

$$\ell n \; r_d = (-E_d/2k) \; 1/T + \ell n \; r_o \; . \qquad (6)$$

This expression is linear if $\ell n \; r_d$ is plotted as a function of inverse temperature. The slope of the line is $-E_d/2k$, while the ordinate intercept is r_o.

III. EXPERIMENTAL APPARATUS AND PROCEDURE

Textured surfaces can be generated by simultaneously sputtering a surface at high energy while seeding it with impurity atoms at low energy. The sputtering can be done in a number of ways, and in this study a broad-beam Kaufman ion source is used. This source produces a low energy (50-1500 eV) high intensity (0-2 mA/cm^2) beam which is neutralized using a thermionic filament immersed in the beam. This system allows a high degree of beam control and a fairly low background pressure ($\sim 10^{-5}$ Torr) in the sputtering region. High vacuum is obtained using a closed-cycle cryopump for an oil-free environment ($\sim 10^{-8}$ Torr base pressure). The vacuum chamber is all stainless steel with hinged access ports for both the ion source and fixturing. Argon is used as the source gas at a typical ion energy of 500 eV and at a current density of 1.0 mA/cm^2. The beam diameter is 5 cm at the ion optics and no beam defining apertures are used. There have been other reported studies which find sputtered aperture material to be an additional impurity at the surface, itself capable of initiating cone formation.[16] The samples are mounted normal to the beam at a distance of 25 cm from the source. They are mounted on a temperature controlled copper holder with a thermocouple mounted directly behind the sample. The sample and the holder are both polished and clamped tightly together. No heat conducting medium is used due to a tendency at high temperatures for that medium (In, for example) to flow or diffuse to the front surface, or sometimes evaporate. Since the power flux is rather low (0.5 W/cm^2), and the samples are typically thin (1 mm), the temperature at the surface can be shown to be at most a few degrees above the measured sample-holder temperature. The holder is constructed in such a way that the

sides of the holder slope away from the sample, reducing possible contamination effects seen by others.[17] For the time development studies, the sample holder was modified so that it could be cooled during or after the sputtering. This allowed faster cooldown times in an already lengthy procedure.

The impurity or seed source consists of a target of the chosen seed material placed in the edge of the ion beam between the ion source and the sample. This target is placed at an angle to the beam such that some of the atoms sputtered from its surface impinge on the sample surface (Fig. 1). The magnitude of the impurity seed flux can be controlled by the amount of the target exposed to the beam and the positioning of the impurity sheet in the beam. Since the impurity source is large compared to the sample (20 cm^2 vs. 1 cm^2), and the target and substrate are typically separated by a few centimeters, the impurity flux to the sample can be considered uniform. Strong gradients in seed flux have been treated earlier.[13] The magnitude of this flux ranges from the materials tested here has been experimentally measured to be from 0.2 to 3 percent of the ion beam flux.

The samples to be textured are either foils or thin sheets and are cut into 1 cm^2 squares. All of the samples for each metal substrate used were cut from a single piece, thus assuring the thickness and purity to be repeatable. All samples, as well as impurity materials, were at least 99.95% pure and were polycrystalline. No attempts were made to determine the crystal structure or to use single crystal samples. Grain boundaries were often visible after sputtering, which allowed some differentiation between crystals. The thicker samples were polished mechanically to an approximate mirror finish, and all samples were then ultrasonically cleaned in Alconox, acetone, then ethanol. The samples

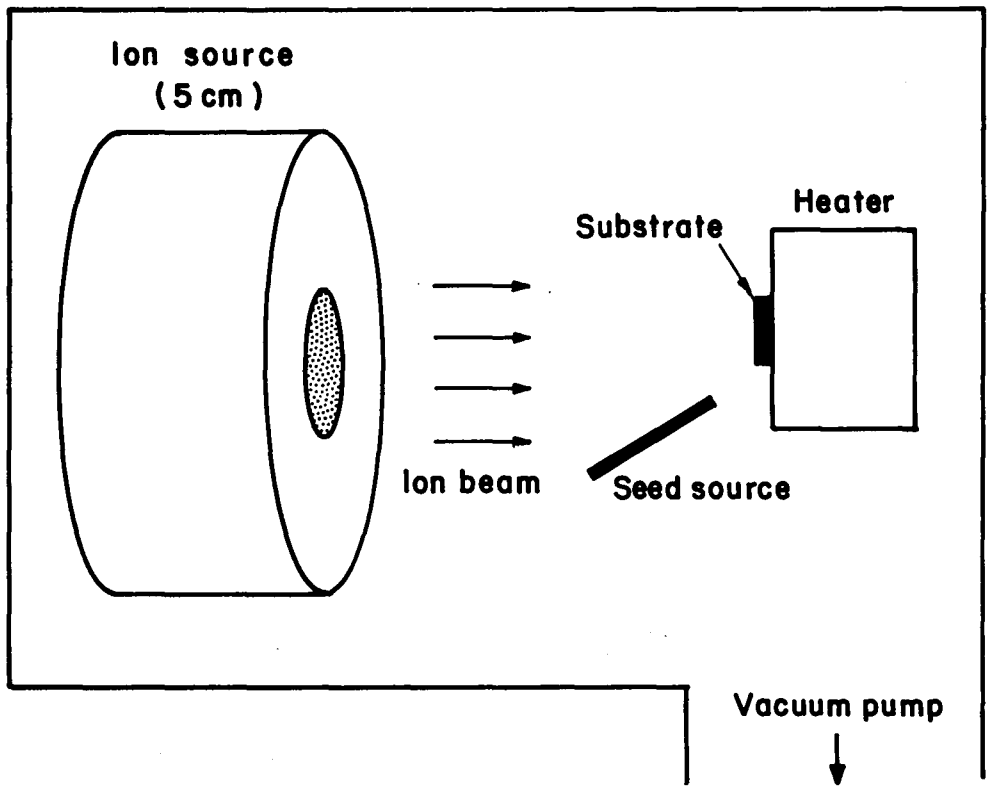

Fig. 1. Schematic of experimental apparatus for microtexturing. The seed source is movable.

were then immediately mounted on the sample holder, evacuated to at least 10^{-7} Torr, and heated to the desired temperature in vacuum.

The subsequent exposure to the ion beam and seed flux varied slightly, depending on the type of experiment. In the time development study the same sample was used for up to 30 sequential exposures. This study will be described in more detail later. The surface diffusion activation energy study used numerous different samples for single exposures. In this study, the samples were simultaneously sputtered and seeded for the times (or doses) necessary to produce steady-state cone structures. The required dose varied from material to material but was kept constant for all measurements on a single material. The doses varied from 5×10^{18} cm^{-2} (15 min.) for Pb to 1.5×10^{19} cm^{-2} (45 min.) for Ni. These doses were sufficient to generate the impurity induced structures while at the same time eroding away the intrinsic conical structures. As will be described in the time-development study, two types of cones can be formed - those due to surface asperities, and those due to the cluster formations of the impurity. The first of these is unrelated to the presence of the impurity, and would produce misleading results in the cone density measurements needed for the activation energy determinations. They are, however, temporary structures which can be removed by sufficient sputtering.

IV. TIME DEVELOPMENT OF SEEDED SPUTTER CONES

The time development of impurity-generated sputter cones has been monitored and described for the first time. These studies entailed sequential exposures (sputtering) and analysis of the same cones over long periods of time - from prior to any sputter-seeding through cone failure and regrowth of succeeding generations of cones. A summary of this work has also been recently published in Radiation Effects Letters.[18]

Time Development of Seeded Sputter Cones on Copper

Cones and pyramids due to sputtering have been generated on surfaces primarily through two methods. One method utilizes relatively high energy ion bombardment (8-50 keV) of ultra-pure crystalline or large grain polycrystalline copper. In many crystal orientations, surface asperities can be sputtered into conical or many-sided pyramidal shapes. This has been variously attributed to either the angular dependence of the sputter yield,[19] or more recently, to a tendency for the solid to minimize surface energy.[20] Generally, with yet only one exception,[21] the features are temporary, and related to the original surface; i.e., they do not reappear during sputtering at greater depths. The second and historically older method of producing these structures is the simultaneous seeding of the sputtered surface of a relatively low level of impurity atoms continuously during sputtering.[2,3,12]

In accord with the diffusional theory, these impurity-generated structures can be formed on a variety of materials, potentially on almost any material at the correct temperature with the appropriate impurity. The elaboration of the time development of these cones is pertinent, particularly to the problem of understanding the underlying mechanisms. The object is not only to be able to generate these

structures on the desired materials, but to have some control over their shapes and sizes as well.

One system was chosen for these experiments, that of Mo impurities on Cu. The basic experiments were: Mo on Cu at 300°C, Mo on Cu at 200°C, and both areas following the removal of the seed source. The particular temperatures were chosen such that one was above the critical temperature (250°C) for diffusion-based coning, and the other was below the critical tempearture.

All of the tests were done in exactly the same way. Cu samples of purity 99.95% were polished to a mirror finish, and cleaned ultrasonically. Areas were then identified in the Scanning Electron Microscope (SEM) that could be repeatably located. The samples were then mounted on a heated sample holder in the vacuum system, evacuated, and brought up to temperature for $\sim$1 hour prior to sputtering. The ion and impurity fluxes were the same in all cases. Following exposure to a specified dose (usually in increments of $1\text{-}2 \times 10^{18}$ ions/cm^2), the sample was removed and re-examined with the SEM, the same area identified through fiducial marks. Following examination, the samples were remounted in the vacuum chamber, heated to the appropriate working temperature for one hour, and re-exposed to the ion beam. This procedure requires exposure to air following each period of sputtering because the ion source and SEM are presently in separate vacuum systems.

The temperature and seeding (impurity) flux were chosen to give a relatively low density of cone structures; the values chosen were obtained through previous experience and systematic variation of the geometry. This facilitated identification of individual cones. In this case the cones were initially separated by roughly 2-6 microns. The results of one series of experiments are shown in Figs. 2(a)-2(cc);

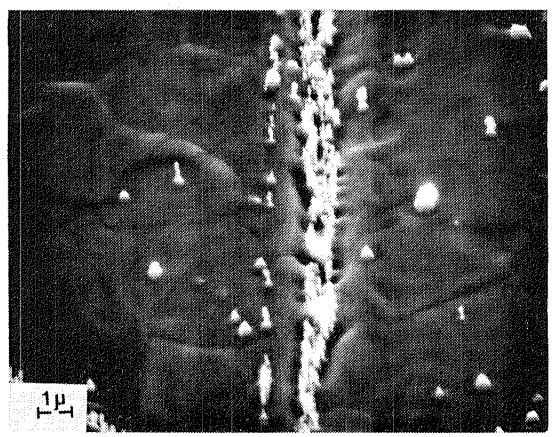

(a) 6 min., 2.2×10^{18} Ar^+/cm^2

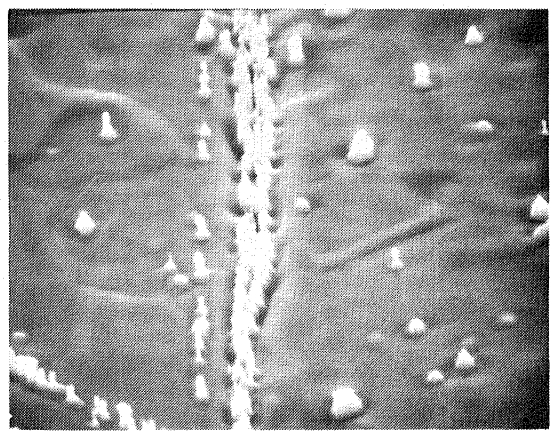

(b) 9 min., 3.4×10^{18} Ar^+/cm^2

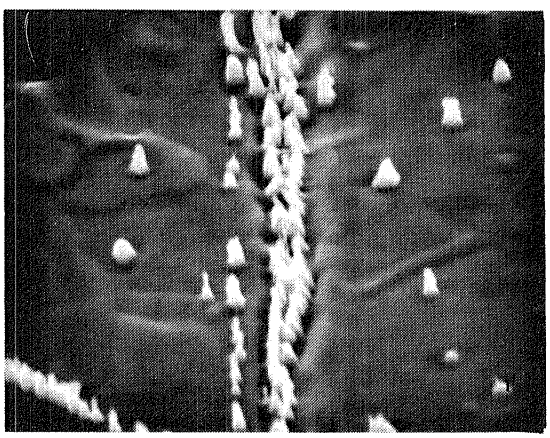

(c) 12 min., 4.5×10^{18} Ar^+/cm^2

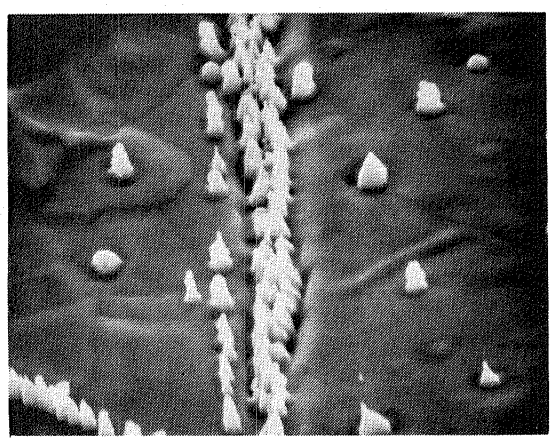

(d) 15 min., 6.8×10^{18} Ar^+/cm^2

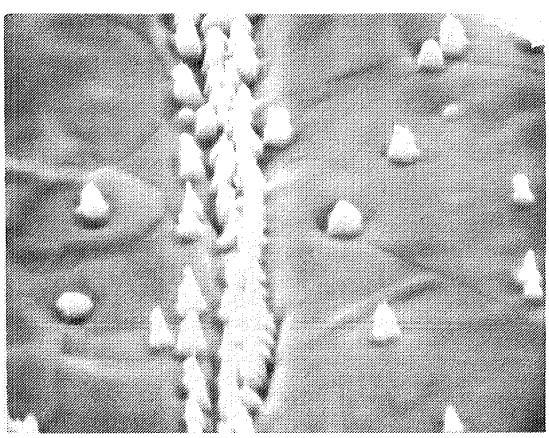

(e) 18 min., 6.8×10^{18} Ar^+/cm^2

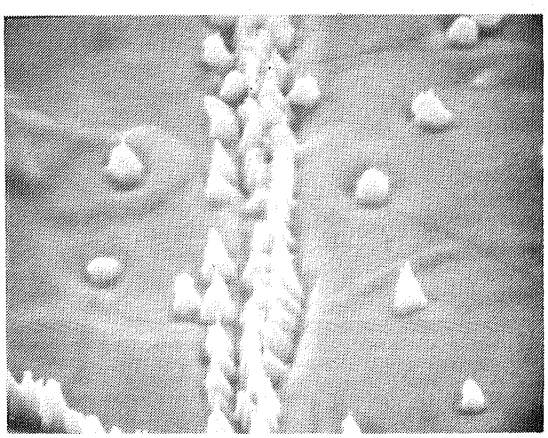

(f) 21 min., 7.8×10^{18} Ar^+/cm^2

Fig. 2. Time development sequence of a single area of Cu seeded with Mo at 300°C. All micrographs taken at the same magnification.

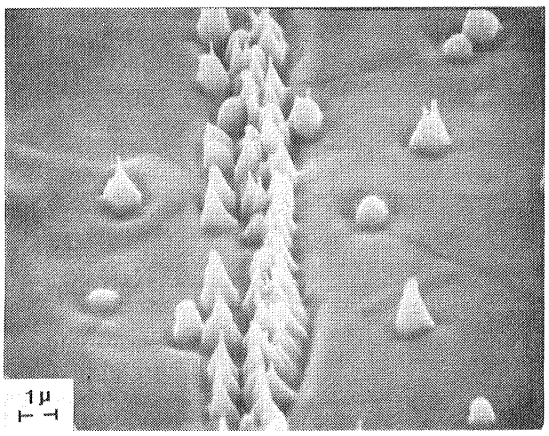

(g) 24 min., 9.0×10^{18} Ar^+/cm^2

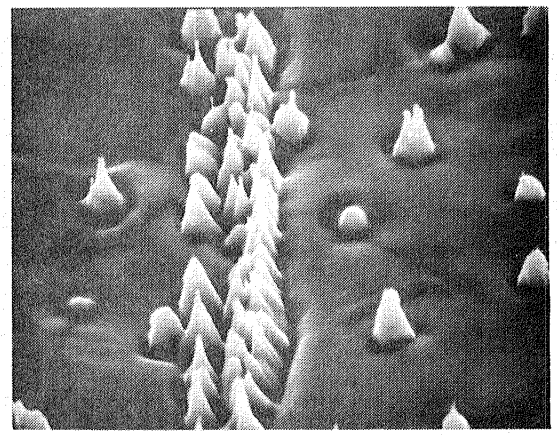

(h) 27 min., 1.0×10^{19} Ar^+/cm^2

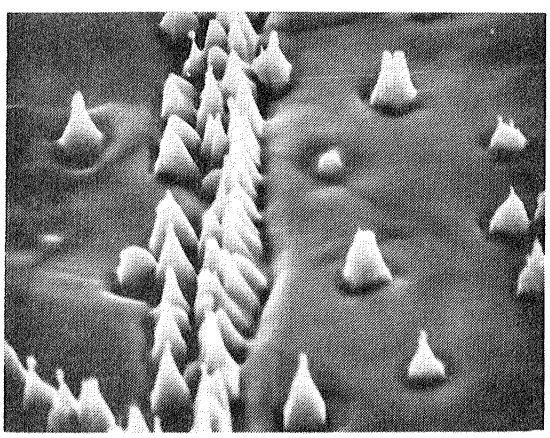

(i) 30 min., 1.1×10^{19} Ar^+/cm^2

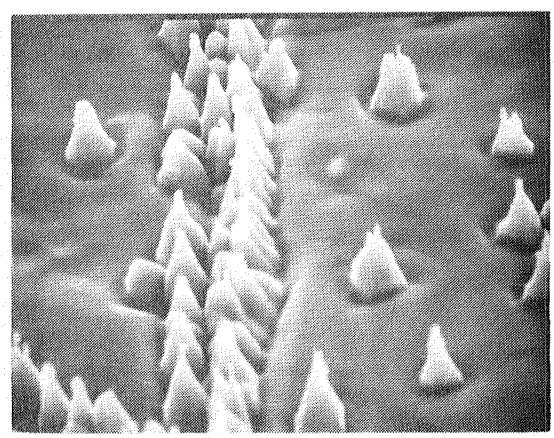

(j) 35 min., 1.3×10^{19} Ar^+/cm^2

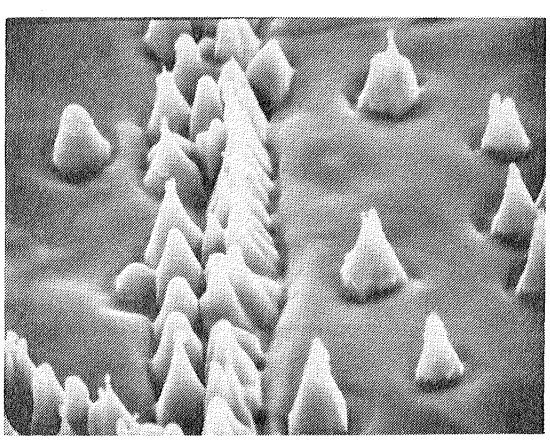

(k) 40 min., 1.5×10^{19} Ar^+/cm^2

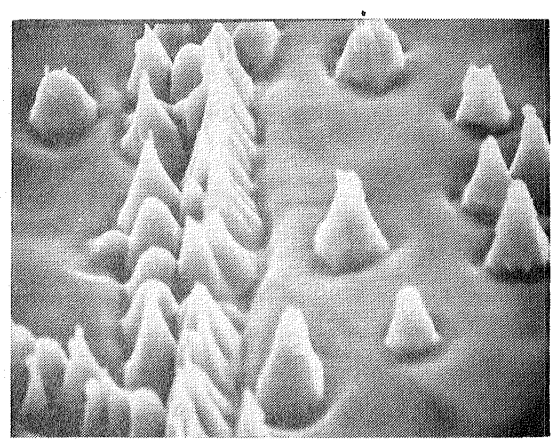

(l) 45 min., 1.7×10^{19} Ar^+/cm^2

Fig. 2. Continued

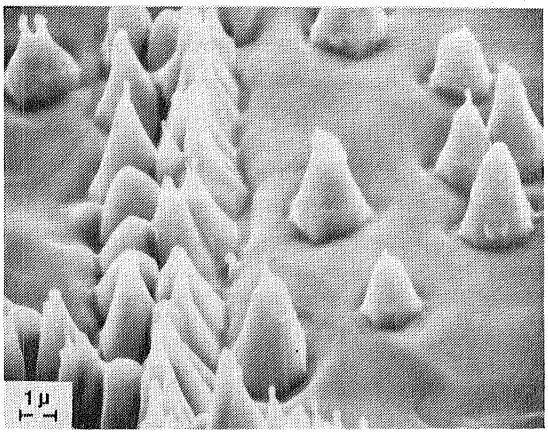

(m) 50 min., 1.9 × 10^{19} Ar^+/cm^2

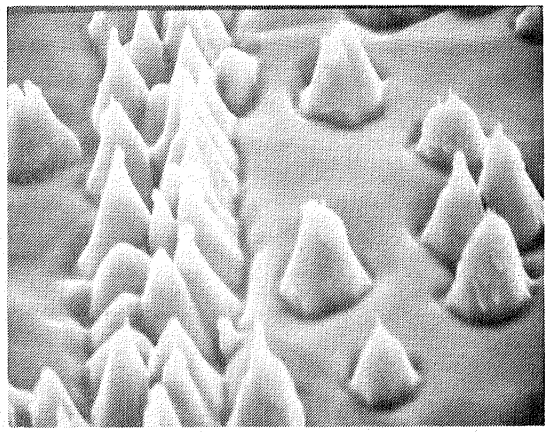

(n) 55 min., 2.1 × 10^{19} Ar^+/cm^2

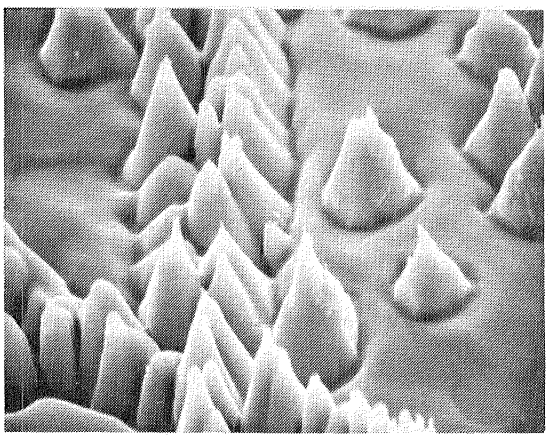

(o) 60 min., 2.25 × 10^{19} Ar^+/cm^2

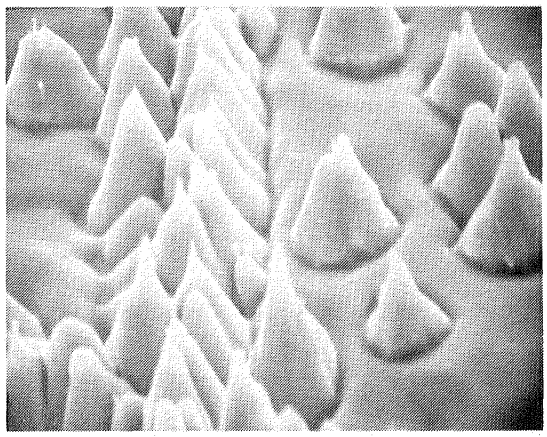

(p) 65 min., 2.4 × 10^{19} Ar^+/cm^2

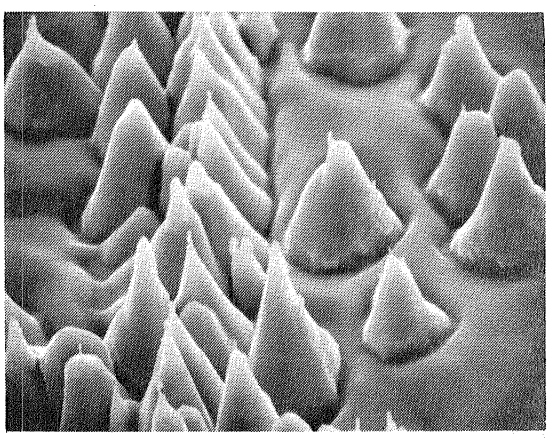

(q) 70 min., 2.6 × 10^{19} Ar^+/cm^2

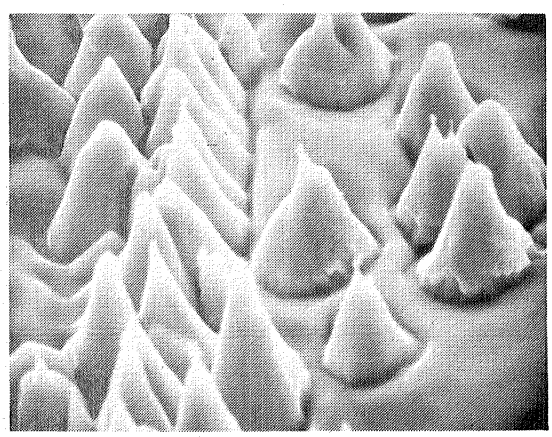

(r) 75 min., 2.8 × 10^{19} Ar^+/cm^2

Fig. 2. Continued

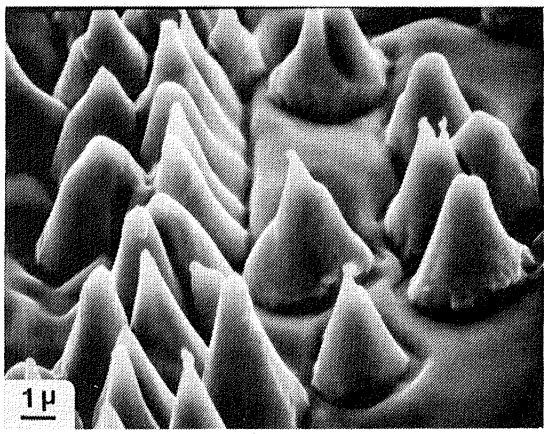

(s) 80 min., 3.0×10^{19} Ar^+/cm^2

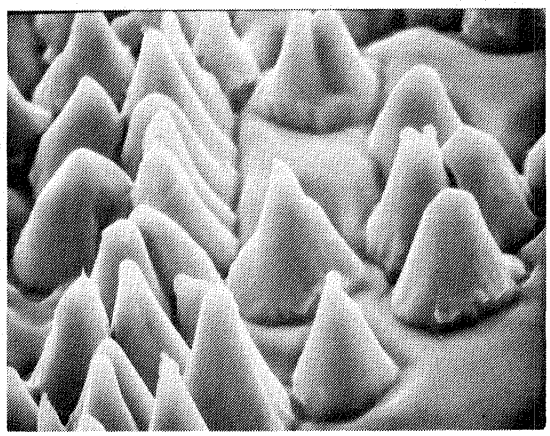

(t) 85 min., 3.2×10^{19} Ar^+/cm^2

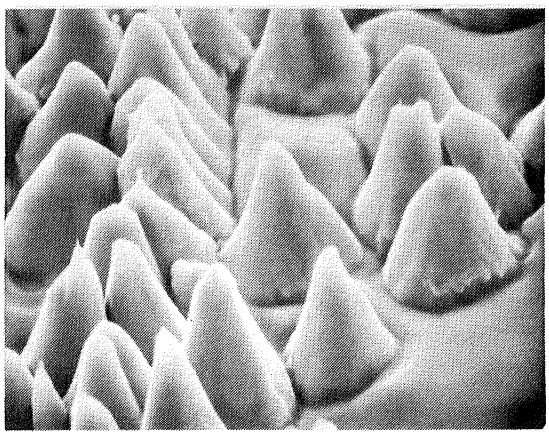

(u) 90 min., 3.4×10^{19} Ar^+/cm^2

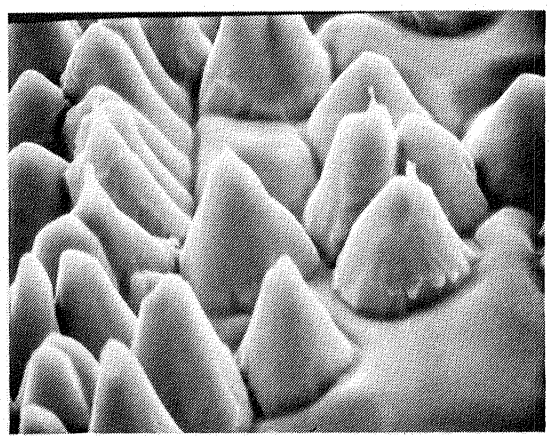

(v) 95 min., 3.6×10^{19} Ar^+/cm^2

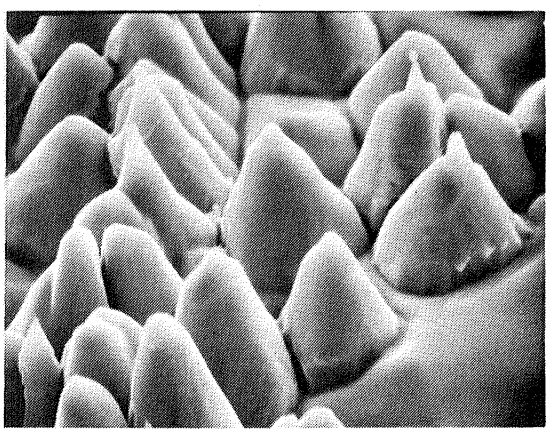

(w) 100 min., 3.75×10^{19} Ar^+/cm^2

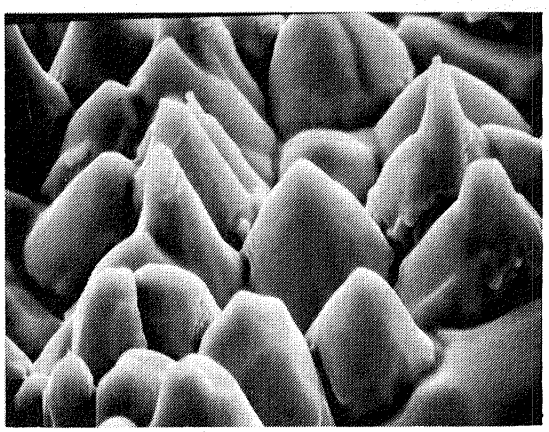

(x) 110 min., 4.1×10^{19} Ar^+/cm^2

Fig. 2. Continued

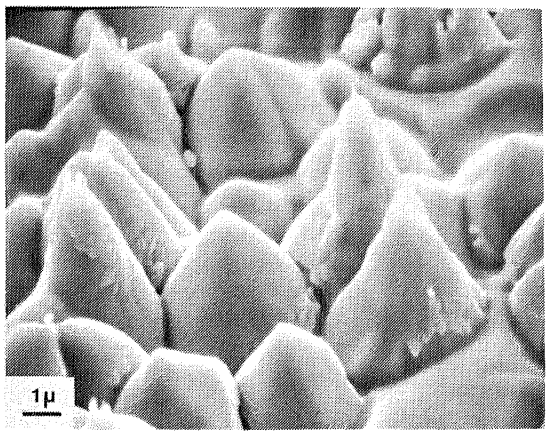

(y) 120 min., 4.5 × 10^{19} Ar^+/cm^2

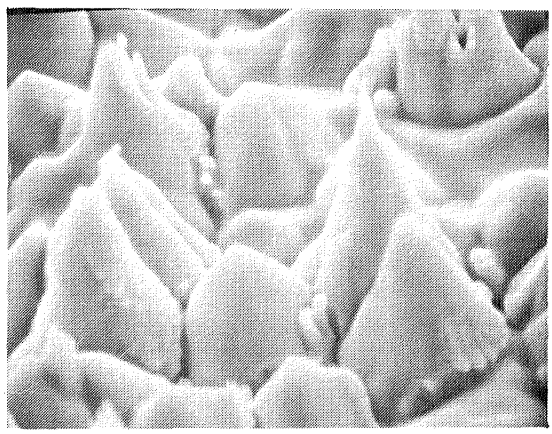

(z) 130 min., 4.9 × 10^{19} Ar^+/cm^2

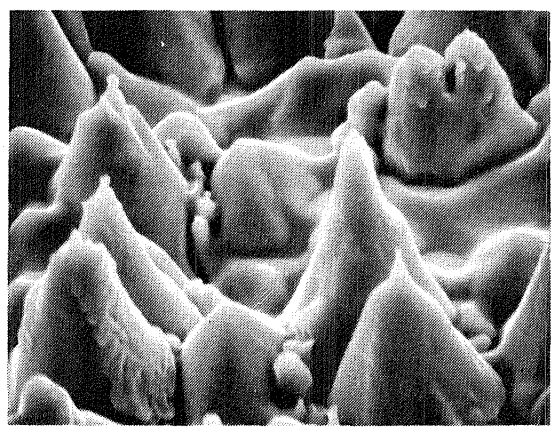

(aa) 140 min., 5.25 × 10^{19} Ar^+/cm^2

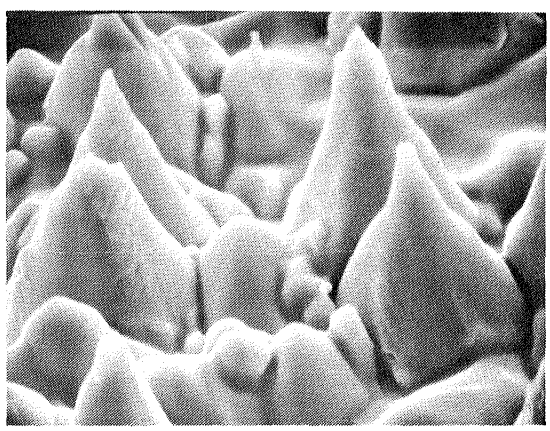

(bb) 150 min., 5.6 × 10^{19} Ar^+/cm^2

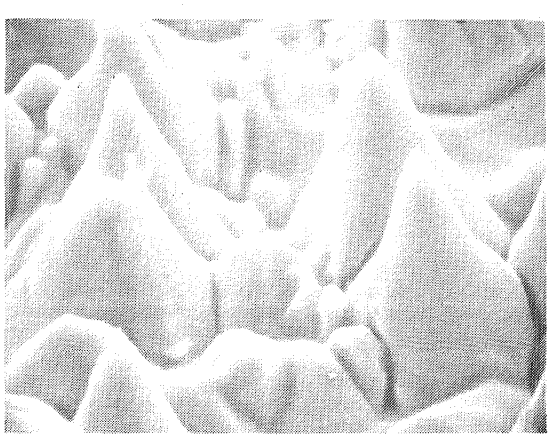

(cc) 160 min., 6.0 10^{19} Ar^+/cm^2

Fig. 2. Continued

the same region of the substrate is shown at successive times during the development of the textured surface. After an initial dose of 1×10^{18} ions/cm^2 at 500 eV, the initial structures generally were of two kinds as shown in Fig. 2(a): large globular forms, and smaller objects that looked somewhat like a "ball-on-a-stick" (BOS). Both of these two initial forms develop into cone-like structures, but the latter is the more stable form. The former structures are apparently due only to asperities at the surface of the copper, rather than the presence of added impurities. This is demonstrated by lowering the temperature of the sample to a point where diffusion is insufficient to initiate cluster formation, in this case 200°C. The globular forms are present at this temperature, but none of the BOS structures. After doses comparable to the 300°C case where this type of structure has been eroded away (2×10^{19} ions/cm^2), the surface at 200°C becomes free of any cone-like structures.

At 300°C, with continued sputtering (5.6×10^{18} ions/cm^2) the BOS structures appear thicker, while the globular forms are being eroded away (Fig. 2(d)). This removal of the asperity related cone structures is characteristic of the descriptions by others.[22] The apex angle increases as the surrounding trough or pit deepens; the eventual result being a slowly broadening (with increasing dose) shallow crater centered on the previous cone site. The thickening of the BOS structures is possibly misleading. Using bulk sputtering rates for copper (15 Å/sec at 1 mA/cm^2 at 500 eV), the planar regions between these structures are eroding such that the thickened forms are actually located below the original structures, which have been sputtered away. With increasing dose on the order of 1.5×10^{19} ions/cm^2, the structures acquire the

more familiar conical shape, and increase in size. Their spacing from peak to peak does not change, but as the bases become larger the areas between the cones decrease. As the cones become larger due to the increased dose, the familiar troughs are seen around the bases (Fig. 2(e)-2(t)). These troughs are never more than 10% of total cone height, and do not seem to be as related to the cone's demise as in the case of non-impurity cones.[22] The troughs are rather flat-bottomed with a steep outer rim. The cones eventually increase in size with continued ion bombardment until adjacent bases touch. As two or more cones grow together due to sputtering, the cone tips remain at approximately the same distance. The cones slowly overlap, with the sides nearest the other cones eroding more slowly than the outer ones. Usually, one cone will eventually dominate the others and become relatively taller. This dominant cone then continues to increase in size until the other cones are absorbed into its sides. The resulting cone can be quite large, its base encompassing the area occupied by the prior cones.

The development of the profile of a single cone from the series given in Fig. 2 is shown in Figs. 3(a) and 3(b). The depth scale is given in microns below the original planar substrate surface. The time scale for total sputtering time is read by extending horizontally the planar base level shown to the right of each successive cone profile. The development of the conical shape and the surrounding trough can be seen as the cone increases in size for approximately 90 min. After this time the cone is clearly being worn away by continued sputtering of the sample.

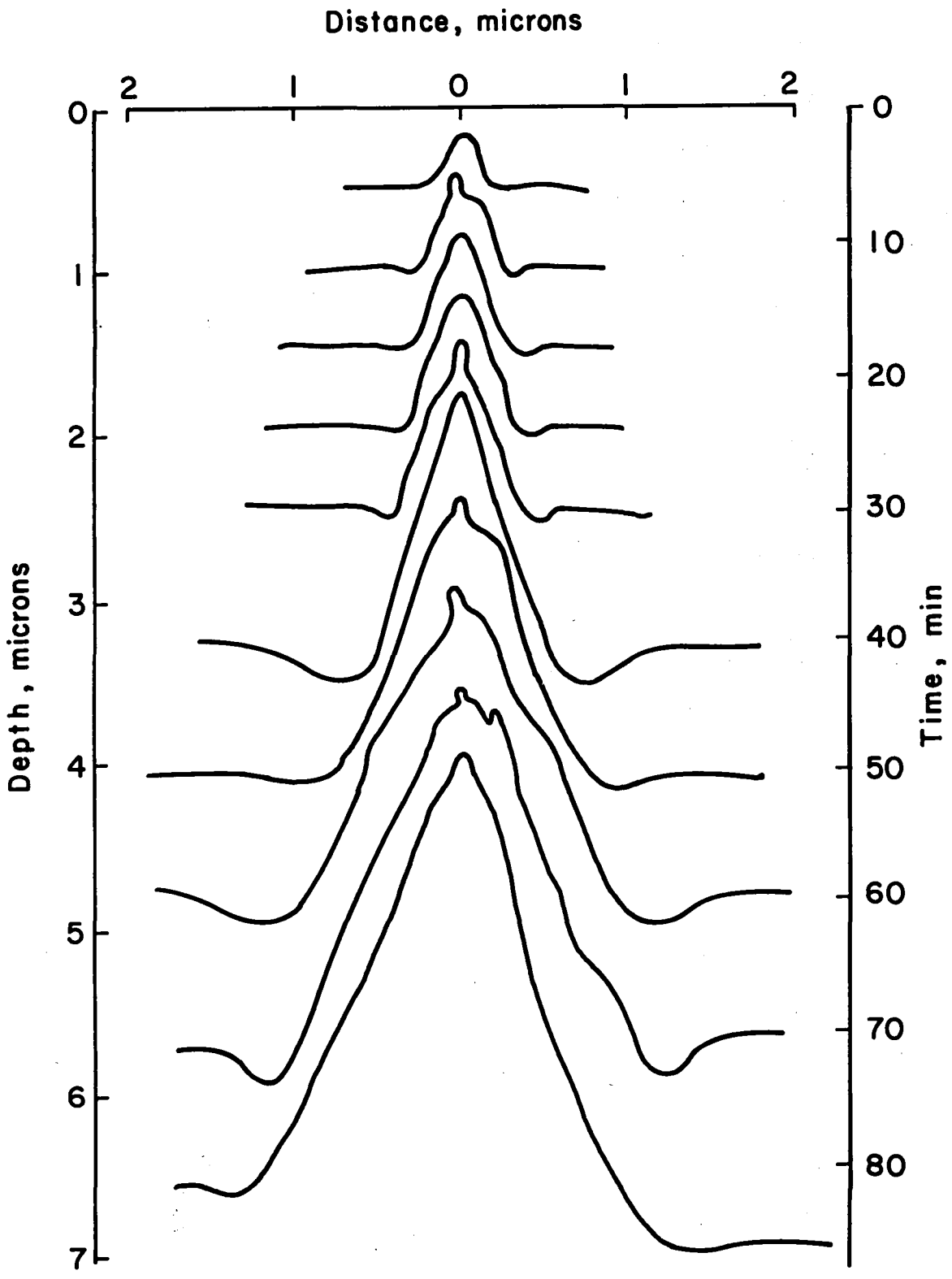

(a) Early development and enlargement.

Fig. 3. Development with time of a single cone beginning at the original planar substrate surface.

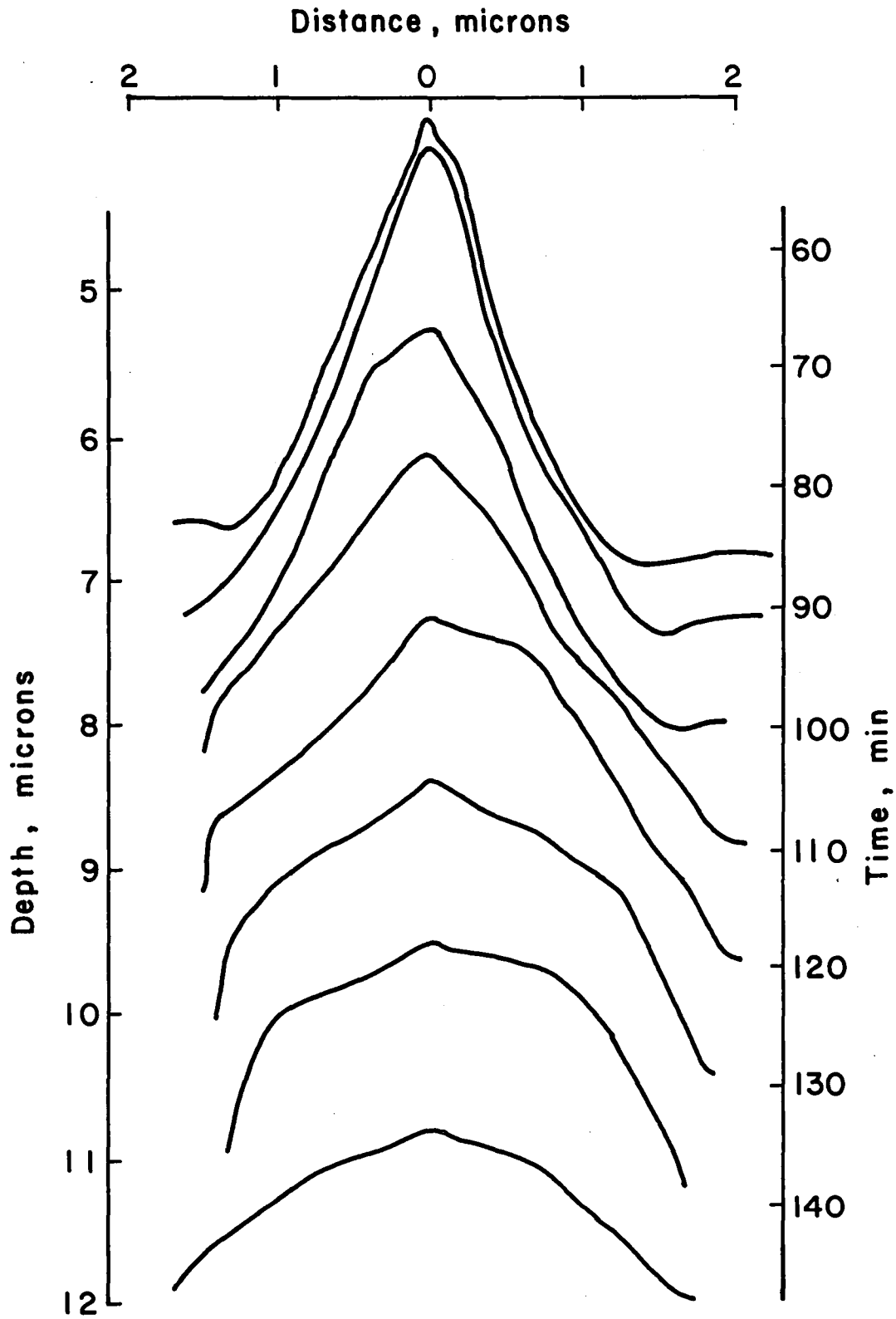

(b) Later development and commencement of removal.

Fig. 3. Continued

Cone Coating

These conical structures have the additional feature of some kind of overlying coating which appears to protect the cones, (i.e., reduce their sputter rate) during cone formation and growth. This coating, while obviously not being a liquid, has the appearance of very viscous fluid on the sides of the cone (Figs. 4(a)-4(b)). From this coating, small protuberances appear occasionally during sputtering, similar in shape and size to the original structures that initiated the cone. These structures were as small as 500 Å in diameter and 200 Å high. Like the original structures, these tended to be replaced (with increased sputtering) by thicker structures below, eventually blending into the side of the cone. Excluding temporary variations due to these ball structures, the cones tended to have a relatively constant apex angle of 45° when corrected for viewing angle.

The cone covering, which usually coats more of the upper 3/4 of the cone, develops a gap at the apex. This gap is accompanied by a flattening of the exposed areas. The gap increases in size until it covers more and more of the upper cone area. The uncovered areas erode more rapidly as evidenced by increasing apex angles. Figures 5(a)-5(d) show an example of a gap developing in the coating on a large, mature cone. One particular cone is marked in the four micrographs with views from both a 45° angle and directly above provided for two different times. In Figs. 5(a) and 5(b) the opening in the covering can be clearly seen. The enhanced erosion of the tip is evident compared to the sides of the cone that are still covered. The uncovered area usually extends eventually over the entire cone, at which time the come erodes into a low ridge. Occasionally this process is accompanied by the growth of new cones at places along the perimeter of this opening in the covering

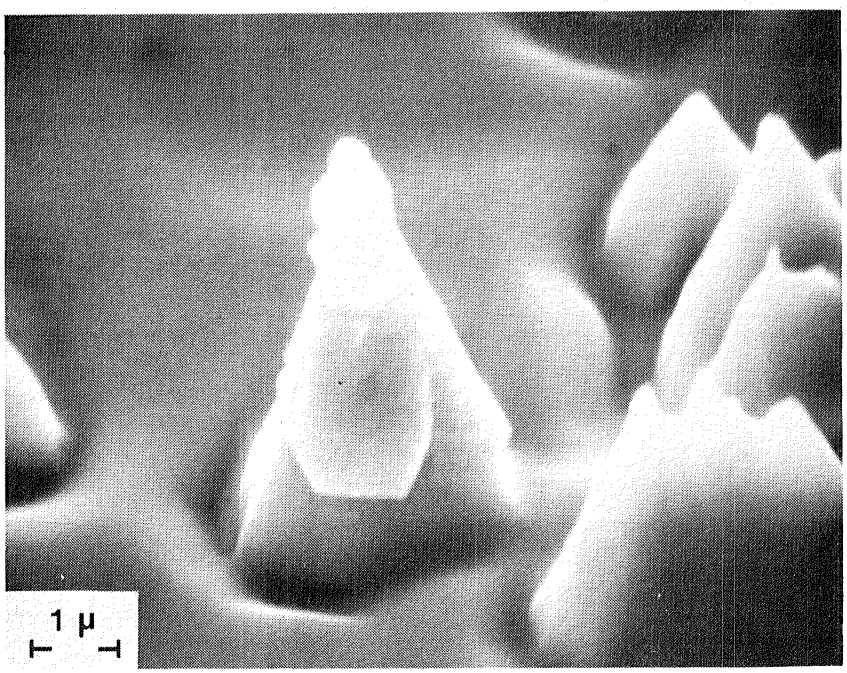

(a) Cu seeded with Mo, 300°C, 2.2×10^{19} cm^{-2}

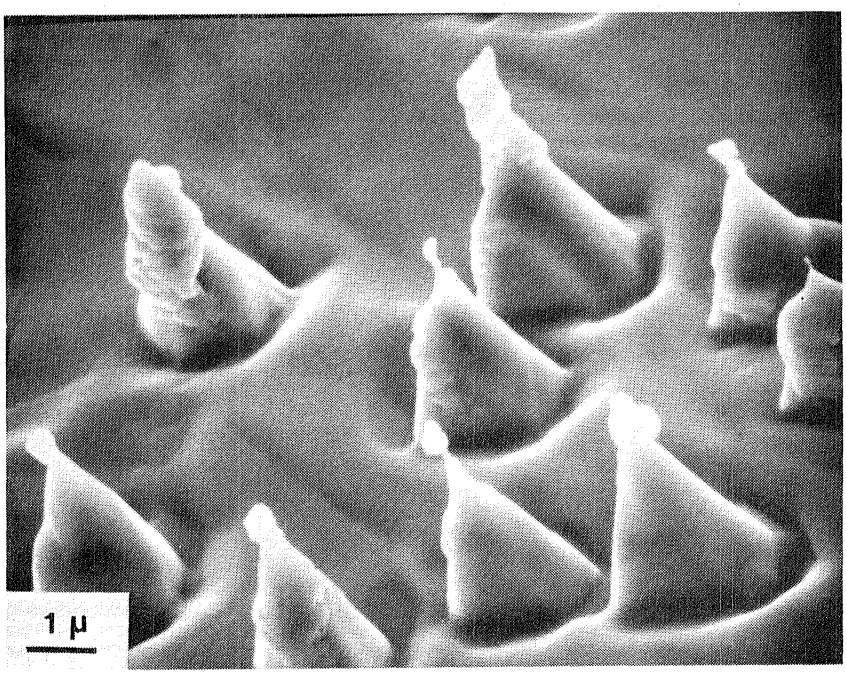

(b) Cu seeded with C, 400°C, 1.5×10^{19} cm^{-2}

Fig. 4. Examples of cones with an overlying coating.

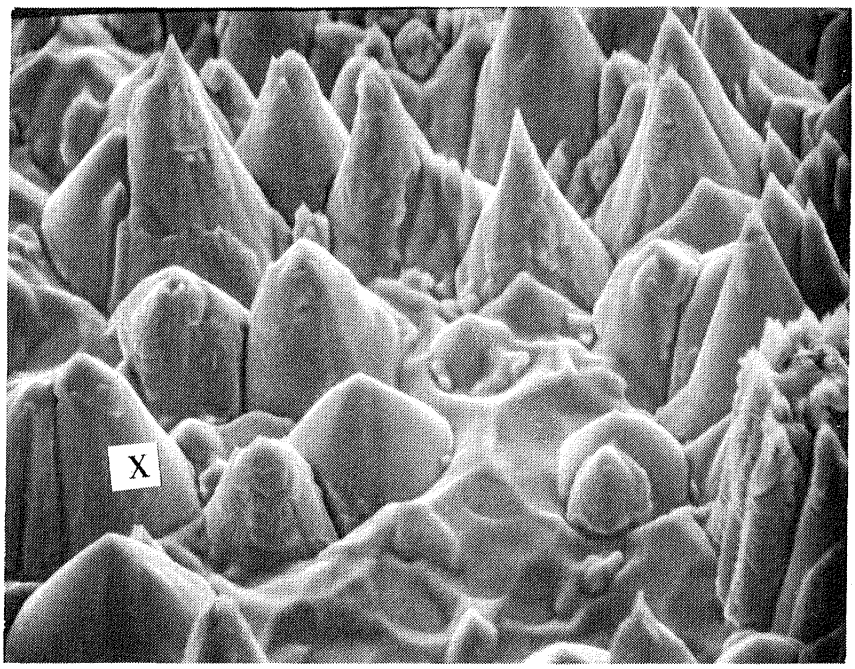

(a) Side view (45°) of cones at 9.7×10^{19} cm^{-2} dose

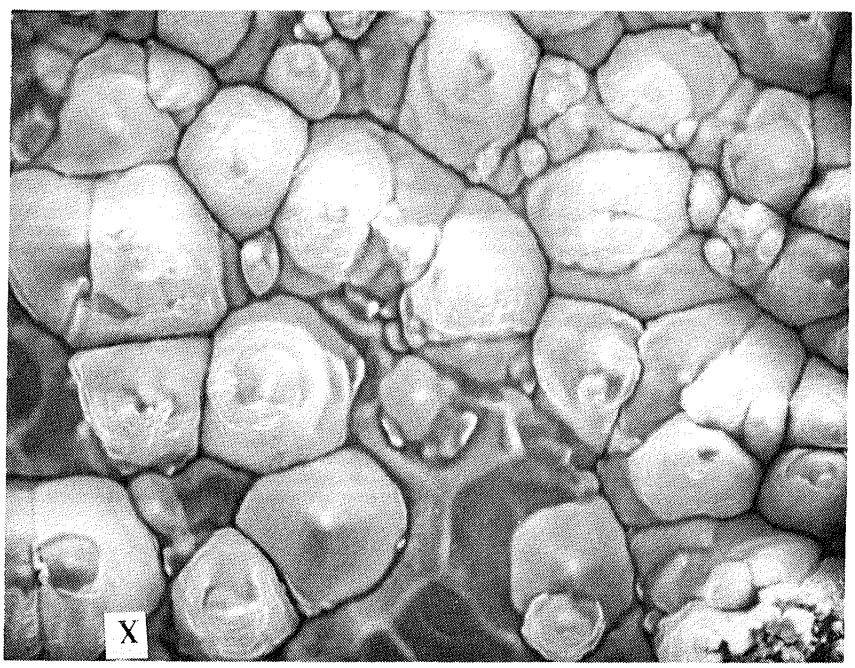

(b) Top view (0°) of cones at 9.7×10^{19} cm^{-2} dose.

Fig. 5. Cones on Cu seeded with Mo at 300°C showing the time development of the opening of the cone covering and the initiation of second generation cones. All micrographs taken at 2400X magnification.

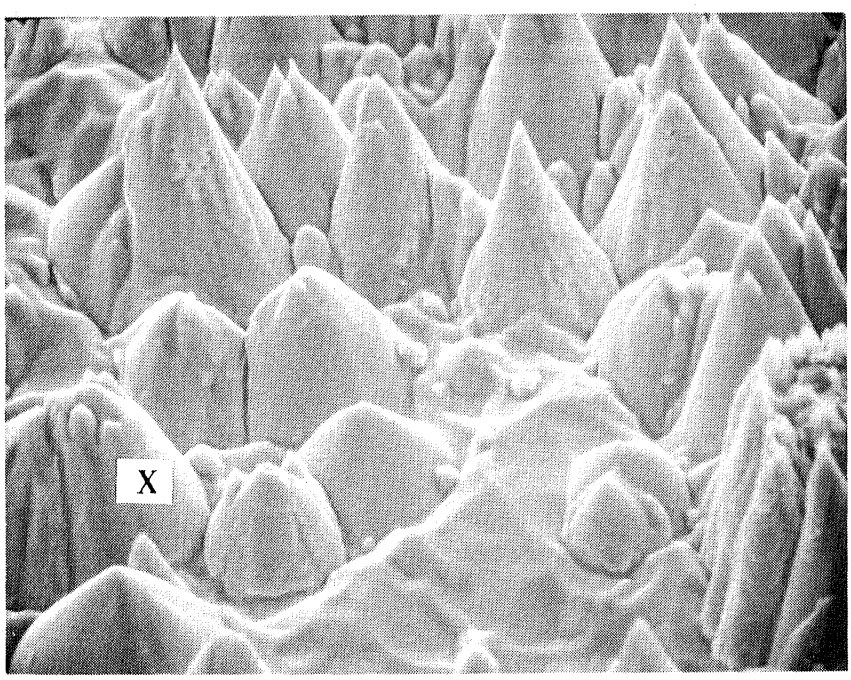

(c) Side view (45°) of cones at 1.05×10^{20} cm^{-2} dose.

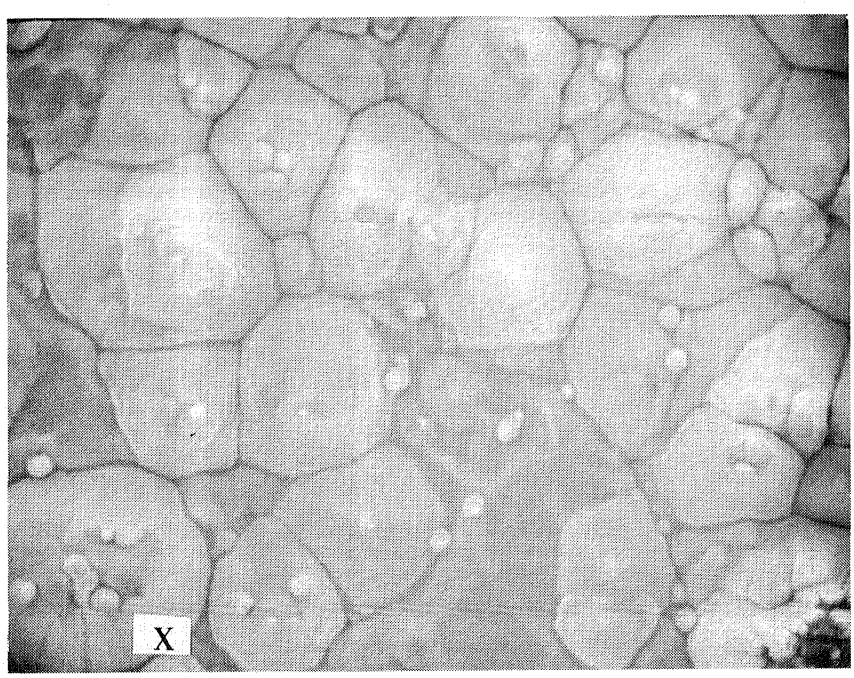

(d) Top view (0°) of cones at 1.05×10^{20} cm^{-2} dose.

Fig. 5. Continued

shown in Figs. 5(c) and 5(d). In a similar experiment with slightly increased impurity seeding rates, the opening in the covering will actually form a circular ridge high on the cone giving the appearance of "hollow cones" that have been observed.[3] The new cones are not always long-lived. They are usually too close together and one will dominate at the expense of the others. The opening of the protective coating does not seem closely related to cone size. Openings were noticed on cones differing in size by a factor of six and many large cones never seemed to develop gaps through the length of the experiment (3×10^{20} ions/cm^2). The openings did not always appear to lead to the destruction of the cone, particularly if the openings were on the side and did not expose the apex. These gaps caused the cones to develop a stepped appearance as the underlying material was eroded. X-ray (energy-dispersive) analysis of the cones, while still in preliminary form, shows the sides of the cones and the tip to be of relatively uniform composition; a few atomic percent of the molybdenum impurity is observed with the majority of the substance being the substrate. Impurity levels were undetectable (<1% atomic) at the base of the cone and in the surrounding area.

It should be noted here that the structures observed in this study were more closely conical than pyramidal. At relatively low doses ($\leq 10^{19}$ ions/cm^2), there were indications of some crystal structure in the bases of the structures. The upper 3/4 of the cone was irregular due to the covering and had no obvious regular or faceted structure. The lower 1/4, however, did occasionally have a regular hexagonal appearance. This structure was lost when the cone interacted with another cone. The structure did not add constructively in the sense that, when two cones combined the resultant structure did not have any regular structure.

While there are certainly some crystalline contributions to the structures, the designation here will continue to be cones rather than pyramids.

The behavior of the cones during sputtering seems implicitly related to observed overlying covering. When this substance is absent, the underlying material erodes relatively quickly. Where this coating has accumulated, the conical structures tend to increase in size. No real growth of the cones was observed in the sense that the heights of the cone tips were always lower than the previous tips when the erosion of the planes between the cones was taken into account. This does not rule out epitaxial growth as possibly evidenced by the coating on the cones. It does indicate, however, that erosion is the dominant mechanism. The increase in size of the cone is attributed to a widening of the cone bases as the planar areas between the individual cones become smaller. The increasing basal dimensions may be a reflection effect, in the same sense that the troughs are formed. The argon ions can be partially reflected from the sides of the cones and cause increased sputtering in the nearby areas. The planar areas have been assumed to have the bulk normal sputtering rate.

Apparently the overlying coating, which is mostly composed of the substrate material with a low percentage of impurity, has a lower sputtering rate than the bulk copper. The coating still has an angle-dependent sputtering yield like most other materials, which tends to stabilize the conical structure. The coating is being constantly replenished by the impurity seeding, although the source of the copper in the coating has not yet been determined. The replenishment of the impurity material is due to both surface diffusion and direct deposition. The diffusional theory[12,13] addresses the nucleation of a cluster on a flat plane which then forms a cone by some mechanism. These present

results can follow the same reasoning, with the small cluster of pure impurity being replaced as sputtering proceeds with a coating having a larger area and a lower concentration of impurity. The observation that the coating seems to recede from a cone top rather than merely fade away suggests a more complicated explanation than diffusion alone.

The effect of surface texture on the effective sputtering yield has been the subject of some discussion.[23,24,25] Some workers notice yield increases, and others decreases; however, most arguments seem to center on the topology. It seems in this case that the apparent reduction is more likely dominated by a material effect evidenced by the protective coating of impurity-substrate material. While we have not measured sputtering yields, Wehner did measure yields for the copper-molybdenum system. Those results found that a copper surface completely covered with molybdenum induced cones at similar temperatures and ion energies had the yield decrease from 2.6 (copper) atoms per ion to 0.9.[3] This seems to agree with the present study, at least qualitatively. For the cones to show any relative growth as compared to the plane, the yield decrease due to this coating must at least offset the yield enhancement due to the increased angle of incidence of ions.

Development Following Seed Removal

In analogy to the time development work, studies have been performed on the time-related loss of cone structures following the removal of the seed material. While the failure mode is somewhat similar to the previously described study, sufficient differences warrent discussion.

Cones were formed to medium size (see Fig. 4(a)) on copper with molybdenum impurities. The molybdenum seed source was then removed, and the sample sputtered and (the same cones) examined sequentially. The primary result is that the cones do not immediately go away. Figure 6

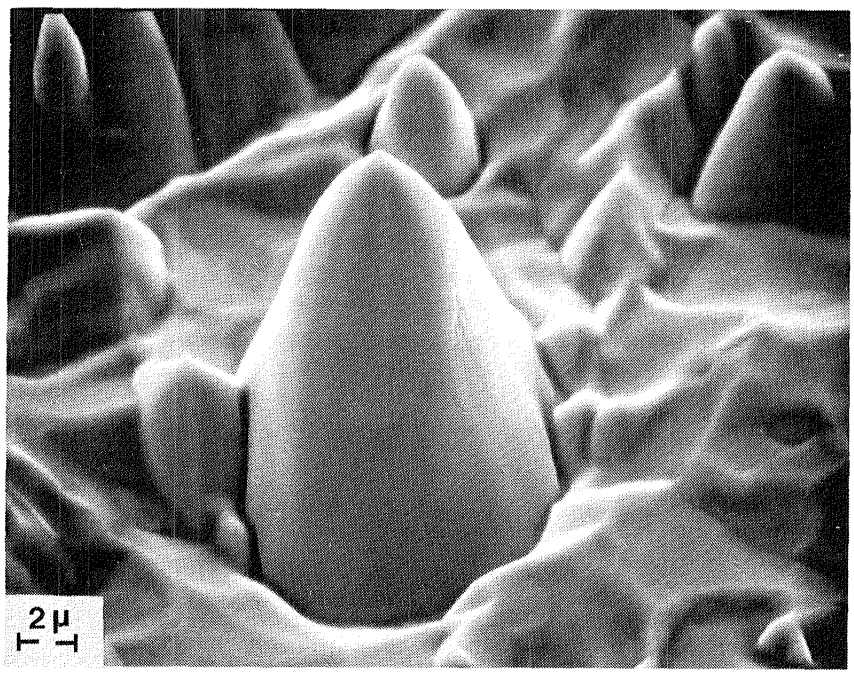

Fig. 6. A cone similar to Fig. 4(a) after removal of the Mo seed source (1.0×10^{20} cm^{-2}). Note relatively steep sides (covered) and flatter top (opened).

is an example of the appearance of a cone after removal of the seed source with the coating substantially removed and more rapid sputter erosion taking place. In fact, growth (erosional growth) continues to occur for up to 200 minutes additional sputtering (at 1 mA/cm^2). This is somewhat misleading, though. The first failures began occurring ∿20 minutes after seed removal. The failure mode was through the previously described opening of the protective coating. On the structures that continued growing, the coating became noticeably thinner with increased sputtering, although it retained liquid-like properties. All of the failures of all of the cones can be attributed to the opening of the protective coating.

V. SURFACE DIFFUSION ACTIVATION ENERGIES

One result of ion beam microetching is the ability to measure the activation energy for surface diffusion of a variety of impurities on many different base materials. In the reported work, 29 different combinations of impurity and substrate have been measured. A paper describing this work has been submitted (APR 1981) to the Journal of Vacuum Science and Technology for publication.

Activation Energy

The activation energy for impurity atom surface diffusion is pictured as the potential barrier height between surface adsorption sites. If this energy remains constant over a few hundred degree temperature range well below the melting point, the random-walk-length of the impurity atom is related to temperature in a simple exponential way. This random-walk-length, which is equated to half the inter-cone spacing, can be plotted logarithmically against inverse temperature in an Arrhenius plot. The slope of the resulting straight line is then proportional to the activation energy (see Eq. (6)). Using this method, the activation energy for impurity atom surface diffusion can be determined without complete knowledge of the numerous other experimental parameters such as ion or impurity flux, sputtering yields, etc. Only temperature was changed from one exposure to the next. Varying other parameters will, according to the model, translate the plotted line uniformly in the vertical or horizontal direction, leaving the slope, and hence the determined activation energy, unchanged.

Experimental Results

In this study, the fundamental measurements are the average cone densities at different temperatures. The density is then converted to an average spacing, the logarithm of which is plotted against inverse temperature, as in Fig. 7. The error bars in the plot are statistical in nature and represent standard deviations from the measured points. The slope is determined by linear regression and is equal to $-E_d/2k$. The results determined in this way are given in Table 1 for the substrates of Cu, Au, Pb, Ni, and Al. The uncertainties are taken as twice the standard deviations of the data points.

The magnitude of the measured activation energies is similar to other measurements by means of field emission[26,27] and by Auger electron spectroscopy.[28] While the field emission values are for materials other than those used in this study, the one Auger measurement is for one of the materials used, Ni. The value given is 0.3 eV for the diffusion of C on Ni,[28] in agreement with values found in this study for other impurities on polycrystalline Ni. The activation energies for surface diffusion appear to be approximately independent of the species of impurity used. Initially one might expect lighter atoms, such as C, to have a much higher mobility than heavier atoms like W or Ta. However, this method measures only the magnitude of the potential barrier between sites. A more mobile atom will have a much longer random-walk length than a less mobile atom, and hence the cone spacing will be increased. The temperature dependence, however, will remain the same because, in the first approximation, both atoms have the same barrier to cross. The difference in mobility will leave the slope in the Arrhenius plot unchanged.

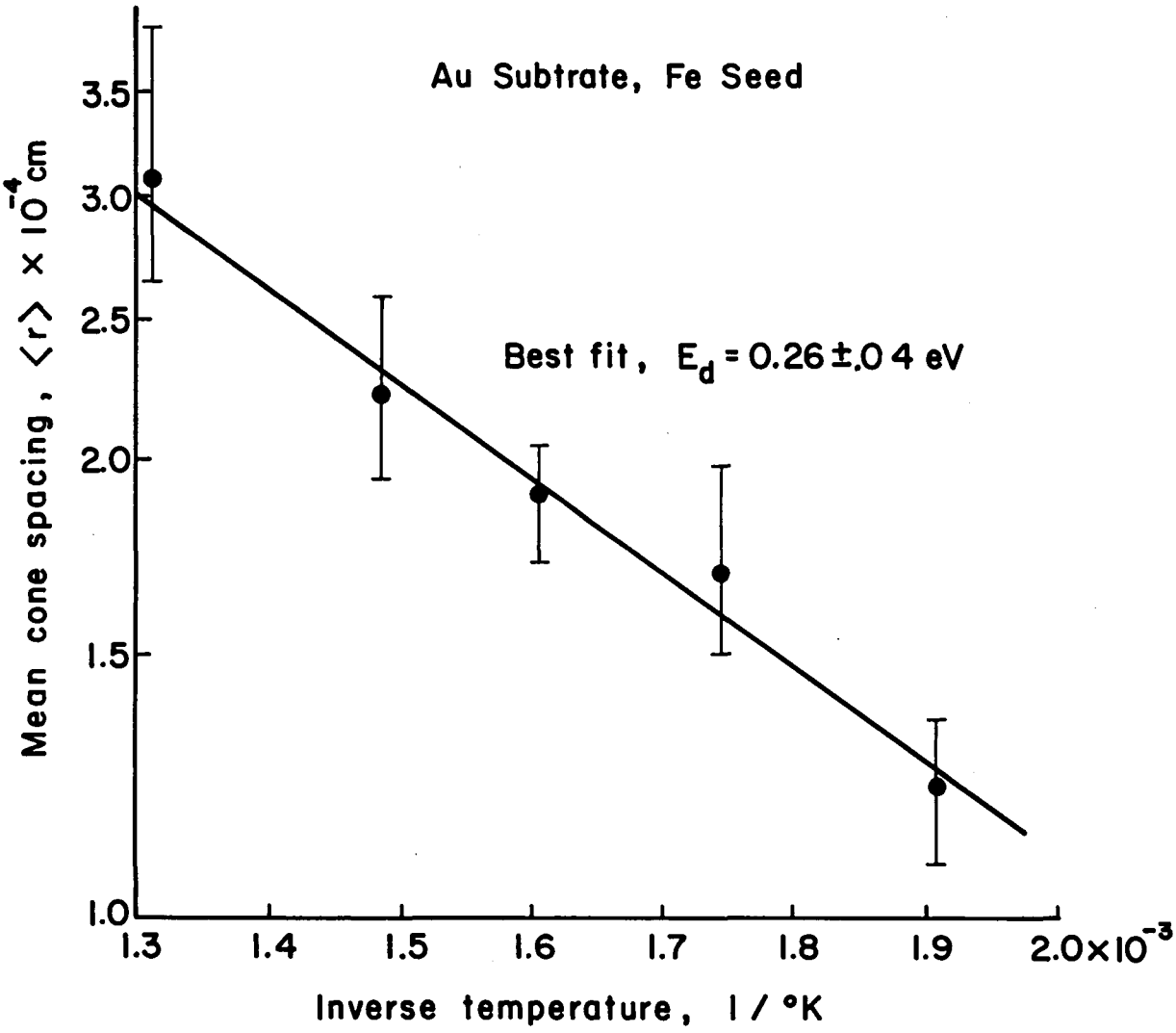

Fig. 7. An example of the type of mean cone spacing versus inverse temperature plot used to determine activation energies.

No significant trend has been found in this work linking the activation energy for surface diffusion to the outer electron shell occupancy of the impurity atom. This was not the case in the field emission studies,[26,27] which linked the activation energy to 5d electron occupancy. While it was not possible in this work to determine the activation energies for a complete row in the periodic table, the measured energies for Ti, Cr, Fe, Ni, and Zn on Cu exhibit no evidence of such a trend.

Table 1. Experimentally Determined Activation Energies for Surface Diffusion.

Seed Materials	E_d(eV) Substrates				
	Cu	Ni	Pb	Au	Al
C	0.42	-	-	-	-
Al	0.35	0.30	-	-	-
Ti	0.41	-	0.32	0.28	0.93
Cr	0.43	-	-	-	-
Fe	0.37	0.32	0.30	0.26	1.0*
Ni	0.46	-	0.33	-	-
Zn	0.31	-	-	-	-
Mo	0.35	0.36	0.31	0.28	1.20
Ta	0.36	-	-	-	0.97
W	0.37	-	-	-	-
Au	0.39	-	-	-	1.04
Cu	-	0.30	0.32	0.29	-
Statistical Uncertainty	±.06	±.06	±.06	±.06	±.09

*Uncertainty ±.15.

VI. OBSERVATIONS ON CONE FORMATION

Additional work has been focused on the crystal structure of cones, critical temperature determinations, and texturing of previously untextured materials. No definative conclusions have yet been reached in these areas, but the present results will be described.

Crystal Structure

As has been mentioned in the Time Development Study, some cones exhibit crystalline features. These are usually only visible from directly above (0° tilt on SEM). The structures take the form of hexagons or parallelograms. (A non-crystalline cone would be expected to have a circular cross-section when viewed from above.) These crystal structures have been observed on Cu, Ni, Au, Pb, and possibly Aℓ. The regular (crystal) structure seems to be present only near the base on the cone - the upper sections being typically coated with the amorphous liquid-like covering. Generally the parallelogram-type structure predominates (Fig. 8). The hexagonal form is relatively rare (Fig. 9), and even in cases of high incedences of crystal structures, the occurrance rate of parallelograms may be only 50%. Typically, when any two or more cones intersect, the resultant boundary will be a straight line when viewed from above, but this is simply geometry. In the present study, crystalline features are evidenced on completely independent structures, i.e., cones separated by at least a diameter.

The crystalline structure can be taken as evidence of the sputter erosion dominated formation of cone structures rather than growth formation. Figures 8 and 9 show separate structures with parallel facets indicating that the separate structures are being sputtered into the same

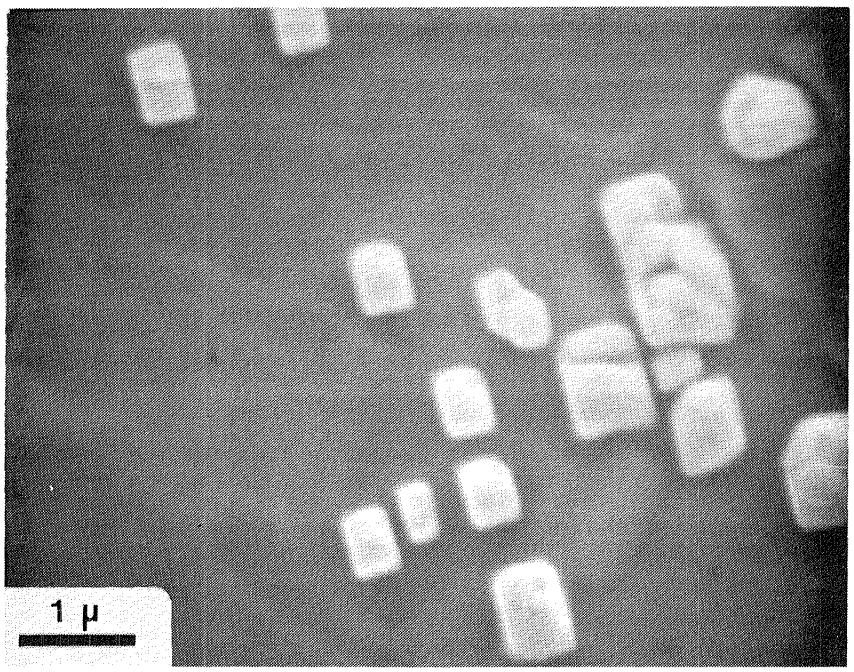

Fig. 8. An example of the parallelogram structure, viewed from above. Au seeded with Fe at 350°C, 1.1×10^{19} cm^{-2}.

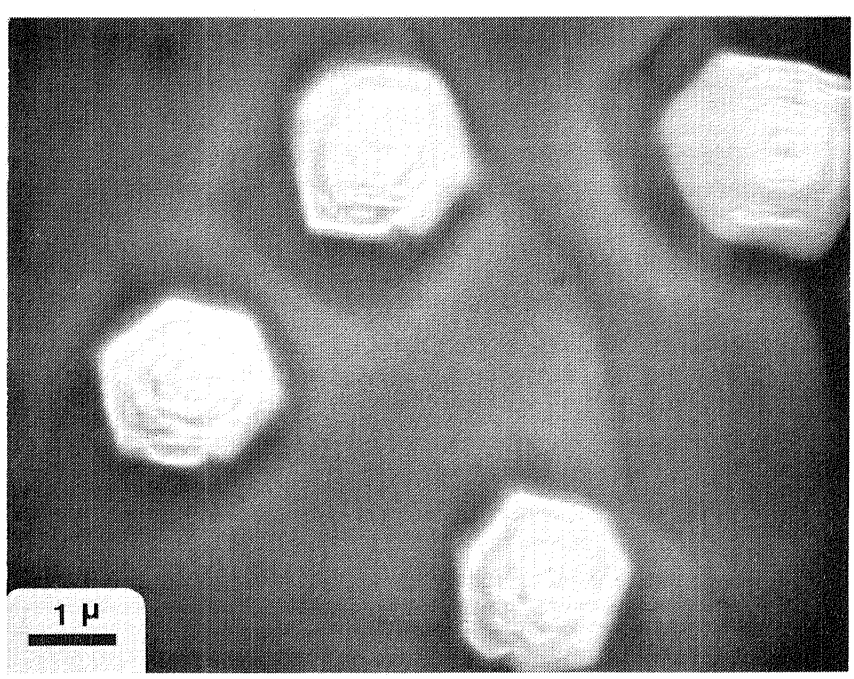

Fig. 9. Hexagonal structure of Cu cones seeded with Mo at 300°C (2.6×10^{19} cm^{-2}), viewed from above.

crystal grain. Occasionally, both parallelogram and hexagonal structures are seen, as in Fig. 10, and often there is an apparent grain boundary separating the two indicating they were eroded into different crystal grains.

In addition, there is a temperature dependence to the occurrence of crystalline features. Typically, they are evident in the range 100-200°C above the critical temperature for surface diffusion driven cone formation.

This study is by no means complete, but appears to be promising. Experimental efforts in this area are continuing.

Critical Temperature

Some critical temperatures for the onset of impurity generated texturing have also been determined. Critical temperatures have much greater uncertainties associated with them than the activation energies but they do not seem to exhibit much variation with seed material. Critical temperature is plotted in Fig. 11 as a function of bulk sputter rate. The bulk sputter rate of the substrate material is for 500 eV Ar^+ ions at a current density of 1 mA/cm^2. The correlation of critical temperature with bulk etch rate appears to be somewhat stronger than the correlation with activation energy. The thermal diffusion model would indicate that the activation energy should dominate the critical temperature. That this does not appear to be the case may prove to be useful both experimentally in predicting texturing properties a priori, and theoretically in suggesting a means of overcoming inadequacies in the present model. It would be very convenient ultimately to be able to relate both the activation energy and the critical temperature to known bulk material properties. Experimental efforts exploring these correlations will be continued.

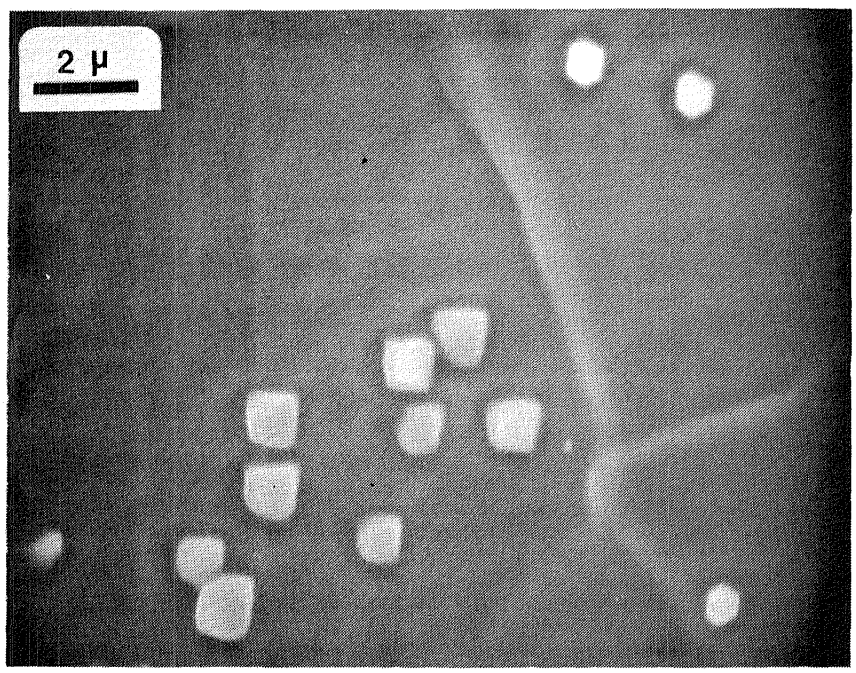

Fig. 10. An example of both parallelogram and hexagonal structures observed on Cu seeded with C at 300°C, viewed from above. Note the grain boundary separating the two regions with different structures.

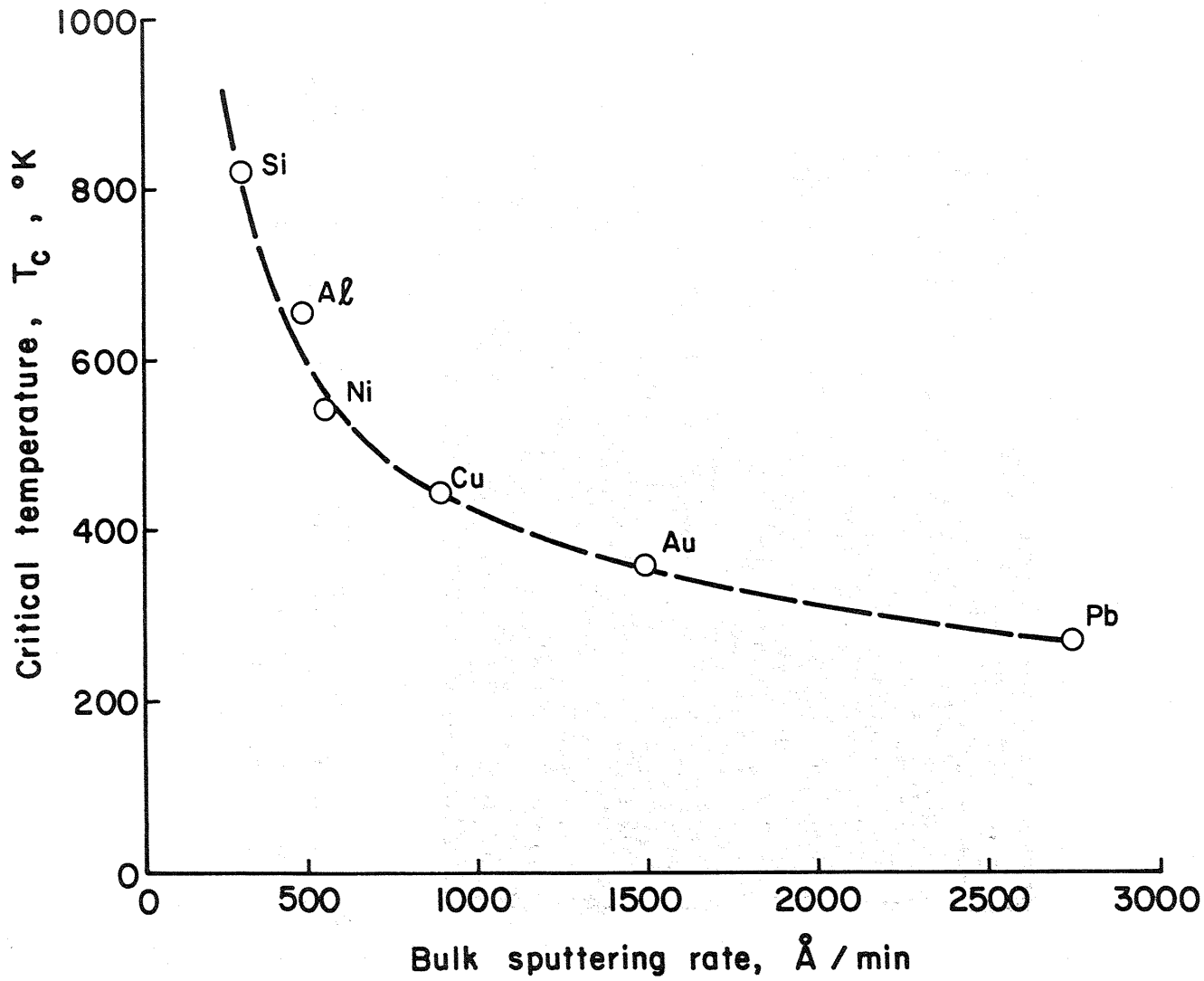

Fig. 11. Correlation of experimentally measured critical temperatures for cone formation with bulk sputtering rates.

Texturing Other Materials

Some effort has gone into the texturing of more difficult materials. These include Ti, A&B, stainless steel, and refractory materials. A&B and stainless steel have been successfully textured, but as yet the refractory metals have not. Work is continuing in these areas.

VII. CONCLUDING REMARKS

Experiments on the detailed time development of individual seeded sputter cones have provided significant insight into the basic processes taking place during ion beam microtexturing. Two cone initiation mechanisms were clearly seen in operation: (1) apparent initial asperities or deposits on the surface that produce short-lived structures that are completely eradicated with sufficient further sputtering, and (2) cone formation at locations where sufficient deliberately deposited seed material has accumulated. For better determination of the average cone density on a surface, it has been found necessary to sputter for a long enough time to be sure that the only remaining cones on the substrate are those formed in response to controlled seeding. This creates some difficulty in verifying predictions from the texturing model on the initial phases of cone growth while the substrate is still fairly flat.

Detailed observation of the role of a coating on cones during formation has generated a number of questions along with the increased understanding of a phase of cone growth that has been largely misunderstood previously. It seems apparent that the coating is a combination of seed and substrate materials that is capable of exhibiting a depressed sputter yield relative to the bulk material. Surface analyses have shown, however, that seed material is only a small fraction of the total. The covering extends over a large fraction of the lateral area of the cone and is not isolated into a small area protecting only the apex. Many observations show clearly that when this coating fails the cone begins to be etched at a faster rate and will ultimately disappear, but so long as the coating remains intact, the cone can continue to increase in size.

There is no significant evidence for cone "growth" beyond the formation of the coating itself; instead, the cones are clearly sputter etched formations at a level lower than that of the original substrate surface. Isolated cones also have been found to exhibit a crystalline symmetry at their bases. Removal of the seed source is followed immediately by the onset of cone failure processes beginning with the thinning and opening of the protective coating. The length of time that cones can remain on the surface after the removal of the seed source depends primarily on the size of the cones at that time.

The ability to experimentally measure activation energies for surface diffusion using ion beam microtexturing has been exploited to measure with a fair degree of confidence the activation energies for 29 different seed-substrate combinations. In all cases the dominant effect appears to be the nature of the substrate material itself with much less effect observed from the use of a very wide variety of seed materials.

The critical temperature for the onset of impurity generated texturing were determined for a number of different materials. A correlation has been found between the critical temperature and the bulk sputtering rate of the substrate. This correlation was not indicated by the earlier theory and represents another area along with the coating material where the existing model does not yet provide sufficient insight.

REFERENCES

1. R. S. Berg and G. J. Kominiak, "Surface Texture by Sputter Etching," J. Vac. Sci. Technol., Vol. 13, No. 1, pp. 403-405 (Jan./Feb. 1977).

2. R. S. Robinson and C. M. Haynes, "Surface Texturing," Industrial Ion Source Technology, NASA CR-135353, pp. 24-75 (Nov. 1977).

3. G. K. Wehner and D. J. Hajicek, "Cone Formation on Metal Targets during Sputtering," J. Appl. Phys., 42, pp. 1145-1149 (Mar. 1971).

4. J. J. Cuomo, J. F. Ziegler, and J. M. Woodall, "A New Concept for Solar Energy Thermal Conversion," Appl. Phys. Lett., Vol. 26, No. 10, pp. 557-559 (May 1975).

5. B. A. Banks, A. J. Weigand, C. A. Babbush, and C. L. Van Kampen, "Potential Biomedical Applications of Ion Beam Technology," AIAA Paper No. 76-1018, AIAA International Electric Propulsion Conference, Key Biscayne, Florida (Nov. 14-17, 1976).

6. W. R. Hudson, "Nonpropulsive Applications of Ion Beams," AIAA Paper No. 76-1015, AIAA International Electric Propulsion Conference, Key Biscayne, Florida (Nov. 14-17, 1976).

7. A. J. Weigand and B. A. Banks, "Ion-Beam-Sputter Modification of the Surface Morphology of Biological Implants," J. Vac. Sci. Technol., Vol. 14, No. 1, pp. 326-331 (Jan./Feb. 1977).

8. W. R. Hudson, "Ion Beam Texturing," J. Vac. Sci. Technol., Vol. 14, No. 1, pp. 286-289 (Jan./Feb. 1977).

9. P. K. Agarwal, E. L. Park and A. J. Weigand, "Ion Beam Texturing of Heat Transfer Surfaces," AIAA Paper No. 81-0670, AIAA/JSASS/DGLR 15th International Electric Propulsion Conference, Las Vegas, Nevada (April 21-23, 1981).

10. C. A. Spindt, "Physical Properties of Thin Film Field Emission Cathodes with Molybdenum Cones," J. Appl. Phys. 46, p. 5248 (1976).

11. R. Forman, "Secondary Electron Emission Properties of Conducting Surfaces with Application to Multistage Depressed Collectors for Microwave Amplifiers," NASA Technical Paper 1097 (1977).

12. H. R. Kaufman and R. S. Robinson, "Ion Beam Texturing of Surfaces," J. Vac. Sci. Technol., Vol. 16, No. 2, pp. 175-178 (Mar./Apr. 1979).

13. R. S. Robinson, "Physical Processes in Directed Ion Beam Sputtering," NASA CR-159567 (March 1979).

14. C. A. Neugebauer, "Condensation, Nucleation, and Growth of Thin Films," in Handbook of Thin Film Technology, pp. 8-3, 8-44 (1970).

15. A. W. Adamson, Physical Chemistry of Surfaces, pp. 372-384 (1976).

16. R. S. Gvosdover, V. M. Efremenkova, L. B. Shelyakin and V. E. Yurasova, "Formation of Cones during Sputtering," Rad. Eff. Vol. 27, p. 237 (1976).

17. R. S. Williams, R. J. Nelson and A. R. Schlier, "Depth Resolution Degradation of Sputter-Profiled InP/$In_xGa_{1-x}As_yP_{1-y}$ Interfaces Caused by Cone Formation," Appl. Phys. Lett., Vol. 36, p. 827, (1980).

18. S. M. Rossnagel and R. S. Robinson, "The Time Development of Impurity-Generated Sputter Cones on Copper," Rad. Eff. Lett., Vol. 58, p. 11 (1981).

19. J. L. Whitton, G. Carter, M. J. Nobes and J. S. Williams, "The Development of Cones and Associated Features on Ion Bombarded Copper," Rad. Eff., Vol. 32, p. 129 (1977).

20. L. T. Chadderton, "The Stability of Cones and Pyramids on Sputtered Surfaces of Copper," Rad. Eff. Lett., Vol. 43, p. 91 (1979).

21. J. L. Whitton, L. Tanovic and J. S. Williams, "The Production of Regular Pyramids on Argon Ion Bombarded Surfaces of Copper Crystals," Appl. Surf. Sci., Vol. 1, p. 408 (1978).

22. O. Auciello, R. Kelley and R. Iricibar, "New Insight into the Development of Pyramidal Structures on Bombarded Copper Surfaces," Rad. Eff., Vol. 46, p. 105 (1980).

23. J. L. Whitton, W. O. Hofer, U. Littmark, M. Braun and B. Emmoth, "Influence of Surface Morphology on the Angular Distribution and Total Yield of Copper Sputtered by Energetic Argon Ions," Appl. Phys. Lett., Vol. 36, p. 531 (1980).

24. D. M. Mattox and D. J. Sharp, "Influence of Surface Morphology on the Low Energy Hydrogen Ion Erosion Yields of Beryllium," J. Nucl. Mat., Vol. 80, p. 115 (1979).

25. J. F. Ziegler, J. J. Cuomo and J. Roth, "Reduction of Ion Sputtering Yield by Special Surface Microtopography," Appl. Phys. Lett., Vol. 30, p. 268 (1977).

26. G. L. Kellogg, T. T. Tsong and P. Cowan, "Direct Observation of Surface Diffusion and Atomic Interactions on Solid Surfaces," Surf. Sci., Vol. 70, p. 485 (1978).

27. D. W. Bassett and M. J. Parsely, "Field Ion Microscope Studies of Transition Metal Adaton Diffusion on (110), (211) and (321) Tungsten Surfaces," J. Phys. D. Appl. Phys., Vol. 3, p. 707 (1970).

28. J. F. Mojica and L. L. Levenson, "Bulk to Surface Precipitation and Surface Diffusion of Carbon on Polycrystalline Nickel," Surf. Sci., Vol. 59, p. 447 (1976).

APPENDIX

TEXTURING BIBLIOGRAPHY

1981 B. A. Banks, "Ion Beam Applications Research - A 1981 Summary of Lewis Research Center Programs," NASA TM 81721.

J. K. G. Panitz, D. J. Sharp and J. T. Healy, "Low Energy Ion Bombardment Evolved Conical Surface Morphologies," J.V.S.T., 18, 1981, p. 405.

S. M. Rossnagel and R. S. Robinson, "The Time Development of Impurity-Generated Sputter Cones on Copper," Rad. Eff. Lett. 58, 1981, p. 11.

S. M. Rossnagel and R. S. Robinson, "Impurity Surface Diffusion Activation Energy Determination Using Ion Beam Micro-texturing," J.V.S.T. (submitted).

S. Rutledge and B. Banks, "Simultaneous Ion Sputter Polishing and Deposition," NASA TM 81679, Jan. 1981.

1980 O. Auciello and R. Kelley, "The Evolution of Pyramidal Structures on Surfaces Bombarded at 60°," Proceedings of Symposium on Sputtering, Austria, 1980, p. 594.

O. Auciello, R. Kelley and R. Iricibar, "New Insight into the Development of Pyramidal Structures on Bombarded Copper Surfaces," Rad. Eff. 46, 1980, p. 105.

H. L. Bay, J. Bohdansky, W. O. Hofer and J. Roth, "Angular Distribution and Differential Sputtering Yields for Low-Energy Light-Ion Irradiation of Polycrystalline Nickel and Tungsten," Appl. Phys. 21, 1980, p. 327.

J. Belson and I. H. Wilson, "Flux Density Equations for Topographical Evolution of Features on Ion Bombarded Surfaces," Rad. Eff. 51, 1980, p. 27.

G. Carter, M. J. Moves, G. W. Lewis and J. L. Whitton, "The Kinetics and Energetics of Sputtering Induced Topography on Solids," Rad. Eff. Lett. 50, 1980, p. 97.

P. M. Curmi, G. L. Harding, "Surface Texturing of Copper by Sputter Etching with Applications for Solar Selective Absorbing Surfaces," J.V.S.T. 17, 1980, p. 1320.

R. Kelley and O. Auciello, "On the Origin of Pyramids and Cones on Ion Bombarded Copper Surfaces," Surf. Sci. 100, 1980, p.

G. W. Lewis, M. J. Notes, G. Carter and J. L. Whitton, "The Mechanics of Etch Pit and Ripple Structure Formation on Ion Bombarded Si and Other Amorphous Solids," Nuc. Instr. Meth. 170, 1280, p. 363.

D. M. Mattox and D. J. Sharp, "Influence of Surface Morphology on the Low Energy Hydrogen Ion Erosion Yields of Beryllium," J. Nuc. Mat. 80, 1979, p. 115.

V. Naundorf and M. P. Macht, "Surface Roughening of Copper by Low Energy Ion Bombardment," Nuc. Instr. Meth. 168, 1980, p. 405.

M. J. Nobes, R. P. Webb, G. Carter and J. L. Whitton, "The Development of Surface Morphology During Sputtering with Spatially Non-Uniform Ion Beams," Rad. Eff. Lett. 50, 1980, p. 133.

P. Sigmund, "Sputtering of Single and Multiple Component Materials," J.V.S.T. 17, 1980, p. 396.

G. N. VanWyk and H. J. Smith, "Crystalline Reorientation Due to Ion Bombardment," Nuc. Instr. Meth. 170, 1980, p. 433.

G. N. VanWyk and H. J. Smith, "The Influence of Ion Bombardment Induced Preferential Orientation on the Sputtering Behavior of Cu," S. Afr. J. Phys. 3, 1980, p. 29.

H. Verbeek, W. Eckstein and R. S. Bhattacharya, "Angular and Energy Distributions of H and He Atoms Backscattered from Gold," J. Appl. Phys. 51, 1980, p. 1783.

R. S. Williams, R. J. Nelson and A. R. Schlier, "Depth Resolution Degradation of Sputter-Profiled InP/$In_xGa_{1-x}As_yP_{1-y}$ Interfaces Caused by Cone Formation," Appl. Phys. Lett. 36, 1980, p. 827.

J. L. Whitton, W. O. Hofer, U. Littmark, M. Braun and B. Emmoth, "Influence of Surface Morphology on the Angular Distribution and Total Yield of Copper Sputtered by Energetic Argon Ions," Appl. Phys. Lett. 36, 1980, p. 531.

1979 O. Auciello and R. Kelley, "On the Relative Stability of Different Topographical Features Developed on Bombarded Copper Surfaces," Rad. Eff. Lett. 43, 1979, p. 187.

O. Auciello, R. Kelley and R. Iricibar, "On the Problem of the Stability of Pyramidal Structures on Bombarded Copper Surfaces," Rad. Eff. Lett. 43, 1979, p. 37.

O. Auciello and R. Kelley, "Further Experimental Evidence on the Importance of Tertiary Effects in the Evolution of Pyramids on Bombarded Copper," Rad. Eff. Lett. 43, 1979, p. 117.

H. L. Bay, J. Bohdansky and E. Hechtl, "Low Energy Sputtering Yields of Nickel as a Function of Ion Mass," Rad. Eff. 41, 1979, p. 77.

R. Behrisch, "Surface Erosion from Plasma Material Interaction," J. Nucl. Mat. 85, 86, 1980, p.

T. Chadderton, "On an Application of the Thermodynamics of the Capillarity of Solids to Surface Topography in Sputtering," Rad. Eff. Lett. 50, 1979, p. 23.

W. Eckstein and H. Verbeek, "Data on Light Ion Reflection," 'Max Planck Institut für Plasmaphysik, IPP 9/32.

H. R. Kaufman and R. S. Robinson, "Ion Beam Texturing of Surfaces," J.V.S.T. 16, 1979, p. 175.

P. Laty, D. Seethanen and F. Degreve, "Microroughness Induced on Solids by Ion Bombardment," Surf. Sci. 85, 979, p. 353.

G. W. Lewis, J. S. Colligon, F. Paton, M. J. Nobes, G. Carter and J. L. Whitton, "The Life Cycle of Copper Cones," Rad. Eff. Lett. 43, 1979, p. 49.

G. M. McCracken, P. E. Stott, "Plasma-Surface Interactions in Tokamaks," Nuc. Fus. 19, 1979, p. 882.

M. J. Mirtich and J. S. Sovey, "Adhesive Bonding of Ion-Beam-Textured Metals and Fluoropolymers," J.V.S.T. 16, 1979, p. 809.

M. Nishi, M. Yamada, S. Suckewer and E. Rosengaus, "Measurements of Sputtering Yields for Low Energy Plasma Ions," Princeton University, PPPL-1521, 1979.

E. L. Park and H. K. Hasuda, "Nucleate Boiling from Ion-Beam Textured Surfaces and from Surfaces with R.F. Plasma Deposited Polymers," Final Report, NASA Grant NSG-3199.

R. S. Robinson, "Physical Processes in Directed Ion Beam Sputtering," Ph.D. Thesis, Colorado State University, 1979.

R. Smith and J. M. Walls, "The Development of Surface Topography During Depth Profiling in Auger Electron Spectroscopy," Surf. Sci. 80, 1979, p. 557.

J. S. Sovey, "Ion Beam Sputtering of Fluoropolymers," J.V.S.T. 16, 1979, p. 813.

A. M. Stoneham, "The Motions of Iron Particles on Graphite," Appl. Surf. Sci. 3, 1979, p. 161.

R. D. Webber and J. M. Walls, "The Structure and Topographical Modification of Surfaces During Depth Profiling," Thin Solid Films 57, 1979, p. 201.

G. K. Wehner, "Whiskers, Cones and Pyramids Created in Sputtering by Ion Bombardment," NASA CR-159549, 1979.

R. Yamada, M. Saidox, K. Sone and H. Ohtsuka, "Dose and Microstructural Effects on Surface Topography Change and Sputtering Yield in Polycrystalline Molybdenum Bombardment with 2 KeV Ne Ions," J. Nucl. Mat. 82, 1979, p. 155.

1978 D. W. Bassett and P. R. Webber, "Diffusion of Single Adatoms of Platinum, Iridium and Gold on Platinum Surfaces," Surf. Sci. 70, 1978, p. 520.

R. Bastasz and G. J. Thomas, "Surface Analysis of Sputtered Stainless Steel," J. Nucl. Mat. 76-77, p. 183.

P. A. Buger, F. Blum and J. H. Schilling, "The Stewart-Thompson Theory Applied to the Glow Discharge," Z. Naturforsch, 33A, 1978, p. 321.

G. Carter, M. J. Nobes and J. L. Whitton, "The Stability of Equilibrium Surface Topography Developed by Sputtering," J. Mat. Sci. 13, 1978, p. 2725.

W. O. Hofer, H. L. Bay and P. J. Martin, "Sputter-Erosion and Impurity Omission from Titanium and Vanadium at Low Energy Ion Bombardment," Max Planck Institut für Plasmaphysik, J. Nuc. Mat. 76-77, 1978, p. 156.

M. Hou, W. Eckstein and H. Verbeek, "Small Angle Backscattering of Hydrogen, Deuterium, Helium and Neon from Single and Polycrystalline Nickel," Rad. Eff. 39, 1978, p. 107.

G. L. Kellogg, T. T. Tsong and P. Cowan, "Direct Observation of Surface Diffusion and Atomic Interactions on Solid Surfaces," Surf. Sci. 70, 1978, p. 485.

U. Littmark and W. O. Hofer, "The Influence of Surface Structures on Sputtering: Angular Distribution and Yield from Faceted Surfaces," J. Mat. Sci. 13, 1978, p. 2577.

M. J. Mirtich and J. S. Sovey, "Optical and Electrical Properties of Ion-Beam-Textured Kapton and Teflon," J.V.S.T. 15, 1978, p. 697.

H. Oechsner, "Sputtered Neutral Particles," Physics of Ionized Gases, ed. B. Navinsek, Univ. of Ljubljana, Yugoslavia, 1978, p. 461.

A. Rizk, "The Effects of Ion Bombarding Ground Surfaces of Stainless Steel in a D.C. Glow Discharge in Ar and Ar+O_2," Vacuum 28, 1978, p. 241.

M. W. Thompson, "Mechanisms of Sputtering," Physics of Ionized Gases, ed. B. Navinsek, Univ. of Ljubljana, Yugoslavia, 1978, p. 289.

G. N. VanWyk and H. J. Smith, "Ion Bombardment Induced Preferential Orientation in Polycrystalline Cu Targets," Rad. Eff. 38, 1978, p. 245.

A. J. Weigand, "The Use of an Ion-Beam Source to Alter the Surface Morphology of Biological Implant Materials," NASA TM-78851, 1978.

A. J. Weigand and M. A. Cenkus, "Mechanical and Chemical Effects of Ion-Texturing Biomedical Polymers," NASA TM-79245, 1978.

J. L. Whitton, "Sputtering as a Means of Depth Profiling," Physics of Ionized Gases," B. Navinsek, ed., Univ. of Ljubljana, Yugoslavia, 1978, p. 335.

J. L. Whitton, L. Tanovic and J. S. Williams, "The Production of Regular Pyramids on Argon Ion Bombarded Surfaces of Copper Crystals," Appl. Surf. Sci. 1, 1978, p. 408.

1977 N. Bibic, T. Nenadovic and B. Perovic, "Sputtering and the Formation of Cones on Cu Based Alloys," Proc. 7th Inter. Vac. Cong. and 3rd Inter. Conf. Solid Surfaces, Vienna, 1977, p. 1485.

G. Carter, J. S. Colligon and M. J. Nobes, "Analytical Modelling of Sputter Induced Surface Morphology," Rad. Eff. 31, 1977, p. 65.

L. T. Chadderton, "On a Relationship Between the Geometry of Cones on Sputtered Surfaces and the Angular Dependences of the Sputter Yields," Rad. Eff. 33, 1977, p. 129.

W. R. Hudson, "Ion Beam Texturing," NASA TM-X-73470 J.V.S.T. 14, 1977, p. 286.

W. R. Hudson, A. J. Weigand and M. J. Mirtich, "Optical Properties of Ion Beam Textured Metals," NASA TM-X-73598, 1977.

W. R. Hudson, R. R. Robson and J. S. Sovey, "Ion-Beam Technology and Applications," NASA TM-X-3517, 1977.

J. L. Whitton, G. Carter, M. J. Nobes and J. S. Williams, "The Development of Cones and Associated Features on Ion Bombarded Copper," Rad. Eff. 32, 1977, p. 129.

J. L. Whitton, G. Carter, M. J. Nobes and J. S. Williams, "Development of Cones and Associated Features on Ion Bombarded Copper," Monograph 77-08, H. C. Oersted Institute, Copenhagen, 1977.

J. F. Ziegler, J. J. Cuomo and J. Roth, "Reduction of Ion Sputtering Yield by Special Surface Microtopography," Appl. Phys. Lett. 30, 1977, p. 268.

1976 B. A. Banks, A. J. Weigand, C. A. Babbush and C. L. Van Kampen, "Potential Biomedical Applications of Ion Beam Technology," NASA TM-X-73512, AIAA Paper 76-1018, Nov. 1976.

R. S. Berg and G. J. Kominiak, "Surface Texturing by Sputter Etching," J.V.S.T. 13, 1976, p. 403.

R. S. Gvosdover, V. M. Efremenkova, L. B. Shelyakin and V. E. Yurasova, "Formation of Cones during Sputtering," Rad. Eff. 27, 1976, p. 237.

W. R. Hudson, "Non Propulsive Applications of Ion Beams," NASA TM-X-73511, 1976; also AIAA Paper 76-1015, 1976.

J. F. Mojica and L. L. Levenson, "Bulk to Surface Precipitation and Surface Diffusion of Carbon on Polycrystalline Nickel," Surf. Sci. 59, 1976, p. 447.

B. Navinsek, "Sputtering-Surface Changes Induced by Ion Bombardment," Prog. Surf. Sci. 7, 1976, p. 49.

O. S. Oen and M. T. Robinson, "Computer Studies of the Reflection of Light Ions from Solids," Nuc. Inst. Meth. 132, 1976, p. 647.

C. A. Spindt, I. Brodie, L. Humphrey and E. R. Westerberg, "Physical Properties of Thin-Film Field Emission Cathodes with Molybdenum Cones," J. Appl. Phys. 47, 1978, p. 5248.

V. E. Yurasova, "Surface and Bulk Phenomena in Single Crystal Sputtering," Physics of Ionized Gases, Univ. of Ljubljana, Yugoslavia, 1976, p. 493.

1975 L. T. Chadderton, "Comments on the Scattering of Charged Particles by Single Crystals, Quasichanneling, Flux Peaking, and Atom Location," Rad. Eff. 27, 1975, p. 13.

W. D. Hofer and H. Liebl, "Depth-Profiling of Cu-Ni Sandwich Samples by Secondary Ion Mass Spectrometry," Appl. Phys. 8, 1975, p. 359.

G. M. McCracken, "The Behavior of Surfaces Under Ion Bombardment," Rep. Prog. Phys. 38, 1975, p. 241.

H. Oechsner, "Sputtering - A Review of Some Recent Experimental and Theoretical Aspects," Appl. Phys. 8, 1975, p. 185.

1974 R. T. K. Baker, P. S. Harris and R. B. Thomas, "Direct Observation of Particle Mobility on a Surface in a Gaseous Environment," Surf. Sci. 46, 1974, p. 311.

J. P. Ducommun, et al., "Development of a General Surface Contour by Ion Erosion: Theory and Computer Simulation," J. Mat. Sci. 9, 1974, p. 725.

K. Tsunoyama, Y. Ohashi, T. Suzuki and K. Tsurouka, "Surfaces of Iron Bombarded with Argon and Oxygen Atoms," Jap. J. Appl. Phys. 13, 1974, p. 1683.

M. J. Witcomb, "Prediction of the Apex Angle of Surface Cones on Ion-Bombarded Crystalline Materials," J. Mat. Sci. 9, 1974, p. 1227.

M. J. Witcomb, "The Development of Ion-Bombardment Surface Structures on Stainless Steel," J. Mat. Sci. 9, 1974, p. 551.

1973 D. J. Barber, F. C. Frank, M. Moss, J. W. Steeds and I. S. T. Tsong, "Prediction of Ion-Bombarded Surface Topographies using Frantic Kinematic Theory of Crystal Dissolution," J. Mat. Sci. 8, 1973, p. 103.

M. Cantagrel and M. Marchal, "Argon Etching in a Reactive Gas," J. Mat. Sci. i, 1973, p. 1711.

G. Carter, J. S. Colligon and M. J. Nobes, "The Growth of Topography During Sputtering of Amorphous Solids," J. Mat. Sci. 8, 1973.

R. S. Nelson and D. J. Mazey, "Surface Damage and Topography Changes Produced During Sputtering," Rad. Eff. 18, 1973, p. 127.

P. Sigmund, "A Mechanism of Surface Micro-Roughening by Ion Bombardment," J. Mat. Sci. 8, 1973, p. 1545.

I. H. Wilson, "The Topography of Sputtered Semiconductors," Rad. Eff. 18, 1973, p. 95.

1971 W. Hauffe, "Development of the Surface Topography on Polycrystalline Metals by Ion Bombardment Investigated by Scanning Electron Microscopy," Phys. Stat. Sol. 4a, 1971, p. 111.

D. M. Mattox and G. L. Kominiak, "Structure Modification by Ion Bombardment During Deposition," J.V.S.T. 9, 1971, p. 528.

G. K. Wehner and D. J. Hajicek, "Cone Formation on Metal Targets During Sputtering," J. Appl. Phys. 42, 1971, p. 1145.

I. H. Wilson and M. W. Kidd, "A Study of Cones Developed by Ion Bombardment of Gold," J. Mat. Sci. 6, 1971, p. 1362.

1970 D. W. Bassett and M. J. Parsley, "Field Ion Microscope Studies of Transition Metal Adaton Diffusion on (110), (211) and (321) Tungsten Surfaces," J. Phys. D. Appl. Phys. 3, 1970, p. 707.

H. E. Cline, "Multineedle Field Emission from the Ni-W Eutectic," J. Appl. Phys. 41, 1970, p. 76.

E. Reuther, J. N. Bradford and A. Van Wigngaarden, "Backscatter Currents from Single Crystals under keV Ion Bombardment," Atomic Collisions Phenomena in Solids, ed. D. W. Palmer, M. W. Thompson and P. D. Townsden, North Holland, Amsterdam, 1970, p. 278.

1969 M. J. Nobes, J. S. Colligan and G. Carter, "The Equilibrium Topography of Sputtered Amorphous Solids," J. Mat. Sci. 4, 1969, p. 730.

A. D. G. Stewart and M. W. Thompson, "Microtopography of Surface Eroded by Ion-Bombardment," J. Mat. Sci. 4, 1969, p. 56.

1968 G. Carter and J. S. Colligan, Ion Bombardment of Solids, Heinemann Educational Books, London, 1968.

D. J. Mazey, R. S. Nelson and P. A. Thackery, "Electron Microscope Examination of the Surface Topography of Ion-Bombarded Copper," J. Mat. Sci. 3, 1968, p. 26.

1942 V. A. Guntherschulze and W. Tollmien, "Neue Untersuchungen über die Kathodenzerstüubung der Glimmentladung," Zeit. Physik 119, 1942, p. 685.

1852 W. R. Grove, "On the Electro-Chemical Polarity of Gases," Phil. Trans. Roy. Soc. 142, 1852, p. 87.

1775 J. Priestley, The History and Present State of Electricity with Original Experiments, Vol. 1, Third edition, Bathurst and Louder, London, 1775.

DISTRIBUTION

	Copies
National Aeronautics and Space Administration Washington, DC 20546	
Attn: RS/Mr. Dell Williams, III	1
RTS-6/Mr. Wayne Hudson	1
RTS-6/Mr. Jerome Mullin	1
MT/Mr. Ivan Bekey	1
National Aeronautics and Space Administration Lewis Research Center 21000 Brookpark Road Cleveland, OH 44135	
Attn: Research Support Procurement Section	
Mr. G. Golinski, MS 500-306	1
Technology Utilization Office, MS 3-19	1
Report Control Office, MS 5-5	1
Library, MS 60-3	2
Mr. N. Musial, MS 500-113	1
Dr. M. Goldstein, Chief Scientist, MS 5-3	1
Mr. T. Cochran, MS 501-8	1
Mr. D. Petrash, MS 501-5	1
Mr. N. Grier, MS 501-7	1
Mr. M. Mirtich, MS 501-7	1
Mr. R. Finke, MS 77-4	1
Mr. B. Banks, MS 501-7	1
Mr. D. Byers, MS 501-7	1
Mr. W. Kerslake, MS 501-7	1
Mr. V. Rawlin, MS 501-7	30
National Aeronautics and Space Administration Marshall Space Flight Center Huntsville, AL 35812	
Attn: Mr. Jerry P. Hethcoate	1
Mr. John Harlow	1
Mr. John Brophy	1
Mr. Robert T. Bechtel	1
Mr. M. Ralph Carruth, Jr.	1
NASA Scientific and Technical Information Facility P.O. Box 8757 Baltimore, MD 21240	
Attn: Accessioning Department	1

National Aeronautics and Space Administration
Goddard Space Flight Center
Greenbelt, MD 20771
Attn: Mr. W. Isley, Code 734 1
Mr. A. A. Vetman 1
Dr. David H. Suddeth 1

National Aeronautics and Space Administration
Ames Research Center
Moffett Field, CA 94035
Attn: Technical Library 1

National Aeronautics and Space Administration
Langley Research Center
Langley Field Station
Hampton, VA 23365
Attn: Technical Library 1
Mr. B. Z. Henry 1

The Aerospace Corporation
P.O. Box 95085
Los Angeles, CA 90045
Attn: Dr. B. A. Haatunion 1
Mr. A. H. Silva 1

The Aerospace Corporation
Space Sciences Laboratory
P.O. Box 92957
Los Angeles, CA 90009
Attn: Dr. Y. T. Chiu 1

Bell Laboratories
600 Mountain Avenue
Murray Hill, NJ 07974
Attn: Dr. Edward G. Spencer 1
Dr. Paul H. Schmidt 1

Boeing Aerospace Company
P.O. Box 3999
Seattle, WA 98124
Attn: Mr. Donald Grim, MS 8K31 1
Mr. Russell Dod 1

Case Western Reserve University
10900 Euclid Avenue
Cleveland, OH 44106
Attn: Dr. Eli Reshotko 1

C.E.N.-F.A.R.
Service Du Confinement Des Plasmas
BP6
92260 Fontenay-Aux-Roses,
FRANCE
Attn: J. F. Bonnal 1

Circuits Processing Apparatus, Inc.
725 Kifer Road
Sunnyvale, CA 94086
Attn: Spencer R. Wilder 1

Commonwealth Scientific Corporation
500 Pendleton Street
Alexandria, VA 22314
Attn: George R. Thompson 1

Computing Center of the USSR Academy of Sciences
Vavilova 40
117333 Moscow, B-333
USSR
Attn: Dr. V. V. Zhurin 1

Comsat Corporation
950 L'Enfant Plaza, S.W.
Washington, DC 20024
Attn: Mr. Sidney O. Metzger 1

COMSAT Laboratories
P.O. Box 115
Clarksburg, MD 20734
Attn: Mr. B. Free 1
Mr. O. Revesz 1

CVC Products
525 Lee Road
P.O. Box 1886
Rochester, NY 14603
Attn: Mr. Georg F. Garfield, Jr. 1

DFVLR - Institut fur Plasmadynamik
Technische Universitat Stuttgart
7 Stuttgart-Vaihingen
Allmandstr 124
WEST GERMANY
Attn: Dr. G. Krulle 1

DFVLR - Institut fur Plasmadynamik
33 Braunschweig
Bienroder Weg 53
WEST GERMANY
Attn: Mr. H. Bessling 1

EG & G Idaho
P.O. Box 1625
Idaho Falls, ID 83401
Attn: Dr. G. R. Longhurst, TSA-104 1

Electro-Optical Systems, Inc.
300 North Halstead
Pasadena, CA 91107
Attn: Dr. R. Worlock 1
Mr. E. James 1
Mr. W. Ramsey 1

Electrotechnical Laboratory
1-1-4, Umezono, Sakura-Mura,
Niihari-Gun
Ibaraki,
JAPAN
Attn: Dr. Katsuya Nakayama 1

Fairchild Republic Company
Farmingdale, NY 11735
Attn: Dr. Domenic J. Palumbo 1

Ford Aerospace Corporation
3939 Fabian Way
Palo Alto, CA 94303
Attn: Mr. Robert C. Kelsa 1

General Dynamics
Kearney Mesa Plant
P.O. Box 1128
San Diego, CA 92112
Attn: Dr. Ketchum 1

Giessen University
1st Institute of Physics
Giessen,
WEST GERMANY
Attn: Professor H. W. Loeb 1

Hughes Aircraft Company
Space and Communication Group
P.O. Box 92919
Los Angeles, CA 90009
Attn: Dr. M. E. Ellison 1
Dr. B. G. Herron 1

Hughes Research Laboratories
3011 Malibu Canyon Road
Malibu, CA 90265
Attn: Mr. J. H. Molitor 1
Dr. R. L. Poeschel 1
Dr. Jay Hyman 1
Mr. R. Vahrenkamp 1
Dr. J. R. Beattie 1
Dr. W. S. Williamson 1

IBM Corporation
Thomas J. Watson Research Center
P.O. Box 218
Yorktown Heights, NY 10598
Attn: Dr. Jerome J. Cuomo 1
Dr. James M. E. Harper 1

IBM East Fishkill
D/42K, Bldg. 300-40F
Hopewell Junction, NY 12533
Attn: Mr. James Winnard 1

Ion Beam Equipment, Inc.
P.O. Box 0
Norwood, NJ 07648
Attn: Dr. W. Laznovsky 1

Ion Tech, Inc.
P.O. Box 1388
1807 E. Mulberry
Fort Collins, CO 80522
Attn: Dr. Gerald C. Isaacson 1

Jet Propulsion Laboratory
4800 Oak Grove Drive
Pasadena, CA 91102
Attn: Dr. Kenneth Atkins 1
Technical Library 1
Mr. Eugene Pawlik 1
Mr. James Graf 1
Mr. Dennis Fitzgerald 1
Dr. Graeme Aston 1

Joint Institute for Laboratory Astrophysics
University of Colorado
Boulder, CO 80302
Attn: Dr. Gordon H. Dunn 1

Kyoto University
The Takagi Research Laboratory
Department of Electronics
Yoshidahonmachi Sakyo-ku
Kyoto 606,
JAPAN
Attn: Dr. Toshinori Takagi 1

Lawrence Livermore Laboratory
Mail Code L-437
P.O. Box 808
Livermore, CA 94550
Attn: Dr. Paul Drake 1

Lockheed Missiles and Space Company
Sunnyvale, CA 94088
Attn: Dr. William L. Owens
Propulsion Systems, Dept. 62-13 1
Mr. Carl Rudey 1

Massachusetts Institute of Technology
Room 13-3061
77 Massachusetts Avenue
Cambridge, MA 02139
Attn: Henry I. Smith 1

New Mexico State University
Department of Electrical and Computer Engr.
Las Cruces, NM 88003
Attn: Dr. Robert McNeil 1

Optic Electronics Corporation
11477 Pagemill Road
Dallas, TX 75243
Attn: Bill Hermann, Jr. 1

Physicon Corporation
221 Mt. Auburn Street
Cambridge, MA 02138
Attn: H. von Zweck 1

Princeton University
Princeton, NJ 08540
Attn: Mr. W. F. Von Jaskowsky 1
Dean R. G. Jahn 1
Dr. K. E. Clark 1

Research and Technology Division
Wright-Patterson AFB, OH 45433
Attn: (ADTN) Mr. Everett Bailey 1

Rocket Propulsion Laboratory
Edwards AFB, CA 93523
Attn: LKDA/Mr. Tom Waddell 1
LKDH/Dr. Robert Vondra 1

Royal Aircraft Establishment
Space Department
Farnborough, Hants
ENGLAND
Attn: Dr. D. G. Fearn 1

Sandia Laboratories
Mail Code 5743
Albuquerque, NM 87115
Attn: Mr. Ralph R. Peters 1

Tektronix, 50-324
P.O. Box 500
Beaverton, OR 97077
Attn: Curtis M. Haynes 1

Texas Instruments, Inc.
MS/34
P.O. 225012
Dallas, TX 75265
Attn: Larry Rehn 1

TRW Inc.
TRW Systems
One Space Park
Redondo Beach, CA 90278
Attn: Dr. M. Huberman 1
Mr. Sid Zafran 1

United Kingdom Atomic Energy Authority
Culham Laboratory
Abingdon, Berkshire
ENGLAND
Attn: Dr. P. J. Harbour 1
Dr. M. F. A. Harrison 1
Dr. T. S. Green 1

University of Tokyo
Department of Aeronautics
Faculty of Engineering
7-3-1, Hongo, Bunkyo-ku
Tokyo,
JAPAN
Attn: Prof. Itsuro Kimura 1

Veeco Instruments, Inc.
Terminal Drive
Plainview, NY 11803
Attn: Norman Williams 1

End of Document